

Complexity of Devonian K-bentonites
in the Appalachian foreland basin:
Geochemical and physical evidence
supporting multi-layered K-bentonite horizons

Abstract of a thesis presented to the Faculty
of the University at Albany, State University of New York
in partial fulfillment of the requirements
for the degree of

Master of Science
College of Arts and Sciences
Department of Earth and Atmospheric Sciences

Lucas Benedict

2004

University at Albany, State University of New York

College of Arts & Sciences

Department of Earth and Atmospheric Sciences

The thesis for the master's degree submitted by

Lucas Benedict

under the title

Complexity of Devonian K-bentonites

in the Appalachian foreland basin:

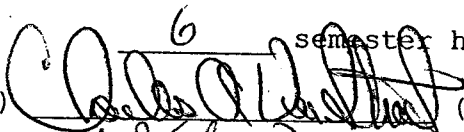
Geochemical and physical evidence

supporting multi-layered K-bentonite horizons

has been read by the undersigned. It is hereby recommended
for acceptance by the Faculty with credit to the amount of

6 semester hours.

(Signed)



(Date)

12/1/04

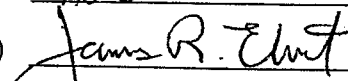
(Signed)



(Date)

1 December 2004

(Signed)

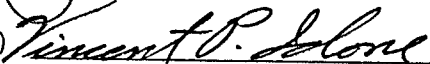


(Date)

11/30/04

Recommended for approval on behalf of the Department.

(Signed)



(Date)

12-1-2004

Recommendation accepted on behalf of the

Graduate Academic Council

(Signed) _____

(Date) _____

ABSTRACT

Detailed analysis of Lower to Middle Devonian K-bentonites in the Appalachian Basin reveals physical and geochemical characteristics within supposed single eruptive event deposits that indicate a more complex depositional history is recorded in many of these volcanic beds. Variations in bedding showing multiple coarse and fine-grained layers within a K-bentonite layer can be seen in some Devonian K-bentonite beds. Microscopic irregularities show variations in the orientation of volcanic grains, and subtle phenocryst layers within a K-bentonite suggest changes in depositional environment where changing water and wave regimes rework and redeposit material on the sea floor. The presence of fossil layers within the same K-bentonite across the basin suggests that the bed records colonization by marine fauna during its deposition. In addition, geochemical inconsistencies within the same layer show evidence that these layers may record more than one eruptive event in a single layer. Based on the analytical methods used in this study many K-bentonite beds are shown to record a more complex preservational and eruptive history than previously thought. By examining physical, petrologic, and elemental geochemical characteristics of these beds, it is seen that many Devonian K-bentonite beds do not in all cases represent the altered remains of single eruptive events.

K-bentonites either (1) contain volcanic material from a single eruptive event, (2) are the result multiple eruptive events, expressed as a subtle, multiple-layered K-bentonite, or (3) a mixing

of volcanic material from a few to many ashfall events where no distinguishable boundary can be seen. The presence of distinctive physical features within layer samples and/or inconsistent trace elemental abundances within phenocrysts from subdivisions of the same bed support the interpretation that more than one eruptive event may have taken place. Data collected in this study strongly supports modern ideas that many Devonian K-bentonites contain more significant volcanic information than previously thought.

Complexity of Devonian K-bentonites
in the Appalachian foreland basin:
Geochemical and physical evidence
supporting multi-layered K-bentonite horizons

A thesis presented to the Faculty
of the University at Albany, State University of New York
in partial fulfillment of the requirements
for the degree of

Master of Science
College of Arts and Sciences
Department of Earth and Atmospheric Sciences

Lucas Benedict

2004

ACKNOWLEDGEMENTS

It would be almost impossible for me to thank everyone and say how much I appreciate the help that I have received from those who have been there for me throughout this entire process. The list could go on forever. Your encouragement and support are greatly appreciated. Thank you.

First, I would like to thank my advisor, Dr. Charles A. Ver Straeten. If Chuck hadn't gone out on a limb to take me as a grad student, who knows where I would be, probably working some dead end job. I have gained so much from being your student and friend, you have no idea. I greatly appreciate all the support that you gave me throughout this quest of mine, especially when I was going through the wonderful later stages of manuscript writing. I hope that I never have to go through that again, but if I do, I know that you are someone that I can talk to. Thanks for being there when I needed someone to vent to.

I would like to thank Dr. George H. Shaw from Union College in Schenectady, New York for all of the help with my analyses. Not only do I appreciate all of the help and guidance throughout this process, but also the ICP-MS analyses were an opportunity for me to use the latest technology and I couldn't pass it up, especially for the price. Thank you for all of the answers to my seemingly endless questions about the processing, separation, and the geochemistry itself. Thanks George, I really can't wait to continue working with you in the future.

Thanks to Dr. James R. Ebert at SUNY College at Oneonta for getting me started in this field. Your enthusiasm for geology, especially in an introductory class like "Intro to the Earth" was what got me to love science. Also, you are the one who got me interested in ash in the first place. Here's to Rickard Hill Road!!

Many thanks go out to Dr. Marian V. Lupulescu for his help with the petrographic analyses and mineral identification for my many thin sections. Your help was greatly appreciated. Also, thanks to Jamie H. MacDonald for the multiple conversations that gave me some new insight and ideas about my data and its implications. Thanks Jamie.

Lastly, I would like to thank my wife and best friend Luci. Without her constant love, support, encouragement, tolerance, and patience I would have never had the strength or ambition to continue with my scholastic endeavors even to get to this point. I Love You Luci! I'm sorry that I put you through hell and back dealing with me as I was writing this thing. It has taken way too long and I know that I put you through so much. I can't tell you enough how much I appreciate it. You have been my inspiration ever since I laid eyes on you. You are so brilliant. This is dedicated to you.

TABLE OF CONTENTS

ABSTRACT	ii
ACKNOWLEDGMENTS	v
TABLE OF CONTENTS	vii
LIST OF TABLES	xii
LIST OF FIGURES	xii
INTRODUCTION	1
GEOLOGIC OVERVIEW	2
PURPOSE OF STUDY	4
PREVIOUS WORK ON DEVONIAN K-BENTONITES	5
FIELD AND LABORATORY METHODS	5
FIELD METHODS	6
ANALYTICAL METHODS	7
Sample preparation	7
Crystal selection and digestion	8
Analytical method	10
Statistical method	10
SAMPLE LOCALITIES	11
NEW YORK LOCALITIES	13
PENNSYLVANIA LOCALITIES	16
VIRGINIA LOCALITIES	20
RESULTS	24
OBSERVABLE PHYSICAL EVIDENCE	24
Field observations	24
Fossil Layers	30
Thin section analyses	34
GEOCHEMICAL EVIDENCE	39
STATISTICAL EVIDENCE	52
DISCUSSION	52
VARIATIONS IN BEDDING	56
Field observations	56
Fossils	58
Thin sections	60
GEOCHEMISTRY OF APATITE PHENOCRYSTS	63
Anomalous geochemistry	66
Seven Fountains, Virginia	66
Tioga B: Seneca Stone Quarry	67

Possible geochemical biases	68
CONCLUSIONS	71
Sprout Brook K-bentonite Cluster	71
The Tioga B K-bentonite	71
Seven Fountains, Virginia	73
SUMMARY	73
REFERENCES AND WORKS CITED	76
APPENDIX A	Sample Localities
	84
A.1: Legend for stratigraphic sections	85
A.2.1: Map of Locality A	86
A.2.2: Photograph of Locality A	87
A.3.1: Map of sites studied at Locality B	88
A.3.2: Photograph of Cherry Valley #1 site	89
A.3.3: Photograph of Cherry Valley #2 site	90
A.3.4: Photograph of K-bentonite beds from Locality B	91
A.4.1: Map of Locality C	92
A.4.2: Photograph of Locality C	93
A.5.1: Map of Locality D	94
A.5.2: Photograph of Locality D	95
A.6.1: Map of Locality E	96
A.6.2: Photograph of Locality E	97
A.7.1: Map of Locality F	98
A.7.2: Photograph of Locality F	99
A.8.1: Map of Locality G	100
A.8.2: Photograph of 7 Fount 3 from Locality G	101
A.9.1: Map of Locality H	102
A.10.1: Map of Locality I	103
APPENDIX B	Geochemical Data
	104
B.1.1: REE concentration values for layer CL# 2(a)	105
B.1.2: Standard deviation values for layer CL# 2(a)	108
B.1.3: REE ratios for layer CL# 2(a)	110
B.1.4: REE concentration values for layer CL# 2(b)	113
B.1.5: Standard deviation values for layer CL# 2(b)	115
B.1.6: REE ratios for layer CL# 2(b)	117
B.1.7: Ce/Pr vs. Dy/Ho ratio plot for layers CL# 2 and COB# 2	119
B.1.8: Mean Ce/Pr vs. Dy/Ho ratio plot for layers CL# 2 and COB# 2	120
B.2.1: REE concentration values for layer CL# 3(a)	121
B.2.2: Standard deviation values for layer CL# 3(a)	123
B.2.3: REE ratios for layer CL# 3(a)	125
B.2.4: REE concentration values for layer CL# 3(b)	127
B.2.5: Standard deviation values for layer CL# 3(b)	129
B.2.6: REE ratios for layer CL# 3(b)	130

B.2.7: REE concentration values for layer CL# 3(c)	131
B.2.8: Standard deviation values for layer CL# 3(c)	133
B.2.9: REE ratios for layer CL# 3(c)	134
B.2.10: REE concentration values for layer CL# 3(d)	135
B.2.11: Standard Deviation values for layer CL# 3(d)	136
B.2.12: REE ratios for layer CL# 3(d)	137
B.2.13: REE concentration values for layer CL# 3(e)	138
B.2.14: Standard deviation values for layer CL# 3(e)	140
B.2.15: REE ratios for Layer CL# 3(e)	141
B.2.16: REE concentration values for layer CL# 3(A)	142
B.2.17: Standard deviation values for layer CL# 3(A)	143
B.2.18: REE ratios for layer CL# 3(A)	144
B.3.1: REE concentration values for layer CL# 4(a)	145
B.3.2: Standard deviation values for layer CL# 4(a)	147
B.3.3: REE ratios for layer CL# 4(a)	149
B.3.4: REE concentration values for layer CL# 4(b)	151
B.3.5: Standard deviation values for layer CL# 4(b)	153
B.3.6: REE ratios for layer CL# 4(b)	154
B.3.7: REE concentration values for layer CL# 4(c)	155
B.3.8: Standard deviation values for layer CL# 4(c)	155
B.3.9: REE ratios for layer CL# 4(c)	156
B.3.10: Ce/Pr vs. Dy/Ho ratio plot for layers CL# 4 and COB# 4	157
B.3.11: Mean Ce/Pr vs. Dy/Ho ratio plot for layers CL# 4 and COB# 4	158
B.4.1a: REE concentration values for layer CL# 8(a)	159
B.4.1b: REE concentration values for layer CL# 8(a)	161
B.4.2a: Standard deviation values for layer CL# 8(a)	163
B.4.2b: Standard deviation values for layer CL# 8(a)	165
B.4.3a: REE ratios for layer CL# 8(a)	167
B.4.3b: REE ratios for layer CL# 8(a)	168
B.4.4a: Statistical information for layer CL# 8(a)	169
B.4.4b: Statistical information for layer CL# 8(a)	169
B.4.5: REE concentration values for layer CL# 8(b)	170
B.4.6: Standard deviation values for layer CL# 8(b)	171
B.4.7: REE ratios for layer CL# 8(b)	172
B.4.8: Ce/Pr vs. Dy/Ho ratio plot for layers CL# 8 and COB# 8	173
B.4.9: Mean Ce/Pr vs. Dy/Ho ratio plot for layers CL# 8 and COB# 8	174
B.5.1: Ce/La vs. Dy/Tb ratio plot for all layers sampled from Locality A	175
B.5.2: Ce/Pr vs. Dy/Ho ratio plot for all layers sampled from Locality A	176
B.5.3: Mean Ce/Pr vs. Dy/Ho ratio plot for all layers sampled from Locality A	177
B.5.4: Nd/Pr vs. Er/Ho ratio plot for all layers sampled from Locality A	178
B.5.5: Nd/Sm vs. Er/Tm ratio plot for all layers sampled from Locality A	179
B.5.6: Gd/Sm vs. Yb/Tm ratio plot for all layers sampled from Locality A	180

B.5.7: Gd/Tb vs. Yb/Lu ratio plot for all layers sampled from Locality A	181
B.6.1: REE concentration values for layer Oak 0-4.5	182
B.6.2: Standard deviation values for layer Oak 0-4.5	184
B.6.3: REE ratios for layer Oak 0-4.5	186
B.6.4: REE concentration values for layer Oak 0-16.0	187
B.6.5: Standard deviation values for layer Oak 0-16.0	189
B.6.6: REE ratios for layer Oak 0-16.0	191
B.7.1: REE concentration values for layer SF 0-5(a)	193
B.7.2: Standard deviation values for layer SF 0-5(a)	194
B.7.3: REE ratios for layer SF 0-5(a)	195
B.7.4: REE concentration values for layer SF 0-5(b)	196
B.7.5: Standard deviation values for layer SF 0-5(b)	198
B.7.6: REE ratios for layer SF 0-5(b)	200
B.7.7: REE concentration values for layer SF 5-8(Clr)	202
B.7.8: Standard deviation values for layer SF 5-8(Clr)	204
B.7.9: REE ratios for layer SF 5-8(Clr)	206
B.7.10: REE concentration values for layer SF 5-8(a)	207
B.7.11: Standard deviation values for layer SF 5-8(a)	208
B.7.12: REE ratios for layer SF 5-8(a)	209
B.7.13: REE concentration values for layer SF 5-8(b)	210
B.7.14: Standard deviation values for layer SF 5-8(b)	212
B.7.15: REE ratios for layer SF 5-8(b)	214
B.7.16: Mean Ce/Pr vs. Dy/Ho ratio plot for layers SF 0-5(a) and SF 0-5(b)	215
B.7.17: Mean Ce/Pr vs. Dy/Ho ratio plot for layers SF 5-8(Clr), SF 5-8(a), and SF 5-8(b)	216
B.7.18: Ce/Pr vs. La/Lu ratio plot for layers CL# 2, CL# 4, and CL# 8 from Locality A	217
B.8.1: Ce/La vs. Dy/Tb ratio plot for all layers sampled from Localities C and D	218
B.8.2: Mean Ce/Pr vs. Dy/Ho ratio plot for all layers sampled from Localities C and D	219
B.8.3: Nd/Pr vs. Er/Ho ratio plot for all layers sampled from Localities C and D	220
B.8.4: Nd/Sm vs. Er/Tm ratio plot for all layers sampled from Localities C and D	221
B.8.5: Gd/Sm vs. Yb/Tm ratio plot for all layers sampled from Localities C and D	222
B.8.6: Gd/Tb vs. Yb/Lu ratio plot for all layers sampled from Localities C and D	223
B.9.1: REE concentration values for layer 7 Fount 1(a)	224
B.9.2: Standard deviation values for layer 7 Fount 1(a)	225
B.9.3: REE ratios for layer 7 Fount 1(a)	226
B.9.4: REE concentration values for layer 7 Fount 1(b)	227
B.9.5: Standard deviation values for layer 7 Fount 1(b)	229
B.9.6: REE ratios for layer 7 Fount 1(b)	230
B.9.7: REE concentration values for layer 7 Fount 1(c)	231
B.9.8: Standard deviation values for layer 7 Fount 1(c)	233
B.9.9: REE ratios for layer 7 Fount 1(c)	234
B.9.10: REE concentration values for layer 7 Fount 3	235
B.9.11: Standard deviation values for layer 7 Fount 3	237

B.9.12: REE ratios for layer 7 Fount 3	238
B.10.1: Ce/La vs. Dy/Tb ratio plot for all layers sampled from Locality G	239
B.10.2: Mean Ce/Pr vs. Dy/Ho ratio plot for all layers sampled from Locality G	240
B.10.3: Nd/Pr vs. Er/Ho ratio plot for all layers sampled from Locality G	241
B.10.4: Nd/Sm vs. Er/Tm ratio plot for all layers sampled from Locality G	242
B.10.5: Gd/Sm vs. Yb/Tm ratio plot for all layers sampled from Locality G	243
B.10.6: Gd/Tb vs. Yb/Lu ratio plot for all layers sampled from Locality G	244
B.10.7: Ce/Pr vs. La/Lu ratio plot for all layers sampled from Locality G	245

LIST OF TABLES

Table 1	Condition and number of crystals selected for ICP-MS analysis.	9
Table 2	Tukey-Kramer HSD values for all volcanic layers collected from Locality A	53
Table 3	Tukey-Kramer HSD values for all volcanic layers collected from Locality D	54
Table 4	Tukey-Kramer HSD values for all volcanic layers collected from Locality G	55

LIST OF FIGURES

FIGURE 1	Sampling sites used in this study.	12
FIGURE 2	Stratigraphic section for Locality A	14
FIGURE 3	Stratigraphic section for Locality B	15
FIGURE 4	Stratigraphic section for Locality B	17
FIGURE 5	Stratigraphic section for Locality C	18
FIGURE 6	Stratigraphic section for Locality D	19
FIGURE 7	Stratigraphic section for Locality E	21
FIGURE 8	Stratigraphic section for Locality F	22
FIGURE 9	Stratigraphic section for Locality G	23
FIGURE 10	Stratigraphic section for Locality H	25
FIGURE 11	Stratigraphic section for Locality I	26
FIGURE 12	Tuffaceous sandstone photograph from Locality G	28
FIGURE 13	Schematic diagram of 7 Fount 1, Locality G	29
FIGURE 14	Three layered K-bentonite photograph from Locality G	31
FIGURE 15	Photograph of brachiopod fossils from Locality E	33
FIGURE 16	Photomicrograph of brachiopod fossil from Locality F	35

FIGURE 17	Photomicrograph from Locality H	37
FIGURE 18	Photomicrograph from Locality G	38
FIGURE 19	REE ratio plots for CL# 2 and COB# 2	40
FIGURE 20	REE ratio plots for CL# 4 and COB# 4	41
FIGURE 21	REE ratio plots for CL# 4	42
FIGURE 22	REE ratio plots for CL# 8 and COB# 8	43
FIGURE 23	Schematic diagram of the Tioga B K-bentonite, Locality D, Locality G	46
FIGURE 24	REE Ratio plots for samples of the Tioga B	47
FIGURE 25	REE Ratio plots for samples from Locality D	48
FIGURE 26	REE Ratio plots for samples from Locality C	50
FIGURE 27	REE Ratio plots for samples from Locality G	51
Figure 28	Heavy versus light REE ratio plot for layers CL# 2, CL# 4, and CL# 8, Locality A	69

INTRODUCTION

The terms K-bentonite, bentonite, and metabentonite describe the isochronous sedimentary layers containing crystals of volcanic origin, including, but not limited to, apatite, biotite, quartz, volcanic glass shards, and zircon that represent the altered remains of airborne volcanic ash deposits. After primary deposition of ash, volcanic glass and other unstable materials within the ash will devitrify and break down during diagenesis to produce combinations of illite-smectite or illite dominated clay layers (Fischer and Schminke, 1984; Königer and Stollhofen, 2001). In addition, K-bentonites are easily affected by multiple stratigraphic factors including erosion, reworking, and mixture with surrounding detrital material by wind, water, gravitational forces, and biological activity (Ver Straeten, 2004). Therefore, the preservation of the primary volcanic ashfall material is solely dependent on the various environmental and biological factors, such as depositional environment, wave action, and biological disruption, throughout the areas where ash is deposited.

K-bentonite layers are extremely important time stratigraphic marker beds. Not only are they regionally correlative across areas of up to hundreds of thousands of km², but they also provide information about regional tectonic history, the chemical characteristics of the host magma, and represent a snapshot of an almost instantaneous window of geologic time (Ver Straeten, 2004).

In this study, K-bentonites in the Appalachian Basin represent the altered Devonian marine ashfall event deposits resulting from

volcanic eruptions during the Devonian Acadian Orogeny. These Devonian layers, and most other K-bentonite beds have historically been interpreted to represent the altered remains of single eruptive ashfall events associated with changes in regional tectonism. Each individual K-bentonite is a distinct layer and presumably contains its own individual and distinguishable characteristics. New studies of Paleozoic K-bentonites in the Appalachian Basin have found that many of these volcanic beds may record a more complex history of ancient volcanism than previously thought (Huff et al., 1999, Ver Straeten, 2004). Examination of multiple volcanic layers from New York, Pennsylvania, and Virginia poses the question, what does a K-bentonite layer actually show us and what do these layers truly represent? If certain K-bentonite beds represent the record of depositional and eruptive histories that are more complex than previously believed, are there K-bentonite layers that represent the simple histories that fit currently accepted interpretations of what K-bentonites represent? By carefully analyzing these layers both sedimentologically and geochemically, one can demonstrate that a number of these layers may record a more complex eruptive history than what has been accepted up to this point.

GEOLOGIC OVERVIEW

Volcanic eruptions associated with the collision of Laurentia and Avalon deposited multiple volcanic ashes, later altered to illite or illite-smectite clay-rich K-bentonites in the adjacent Appalachian foreland basin during the Acadian Orogenic event (Dennison, 1983, 1986; Dennison and Textoris, 1970, 1978, 1987;

Smith et al., 1988; Shaw et al., 1991; Ver Straeten, 1992; Brett and Ver Straeten, 1994; Ver Straeten, 1996; Ver Straeten, 2001; Ver Straeten, 2004). Lower to Middle Devonian aged sediments within the Appalachian Basin were deposited in predominantly marine environments containing both deep and shallow waters with varying physical and biological characteristics as the landmasses collided. The ash beds, deposited with marine sediments, have altered to either illite or illite-smectite dominated clays as a result of the alteration of unstable volcanic glass contained within the deposits as the bed began diagenetic alteration after initial deposition (Hosterman and Whitlow, 1983). Since these beds have a better chance of being preserved in the marine environments of the basin as opposed to terrestrial environments, these beds give us an idea of the volcanic history of orogenic events as these events progressed (Köninger and Stollhofen, 2001).

The Acadian Orogeny consisted of four major cycles of tectonic uplift and resulting subsidence due to crustal loading during episodes of increased tectonic activity and consequent quiescence from the early Devonian to the early Mississippian (Ettensohn, 1985). Collision between Avalon and Laurentia created an orogenic belt extending from southeastern Maritime Canada down through to the southeastern United States, described from the records of tectonism and basinwide sedimentation contained within many of the rocks found within the Appalachian Basin (Osberg et al., 1989; Ettensohn, 1985).

The volcanic beds in this study span roughly 30 million years of the Early to Middle Devonian portion of geologic time. Many of

the beds occur in distinct clusters of K-bentonites that represent active changes in tectonism in the Appalachian basin and surrounding areas during the Devonian (Ver Straeten, 1996, 2004). These beds range in age from 408 +/- 1.9 Ma to 390.0 +/- 0.5 Ma (Roden et al. 1990, Tucker et al., 1998). These beds are the lower Emsian Sprout Brook K-bentonites, and two lower Eifelian Tioga suites of K-bentonites.

PURPOSE OF THIS STUDY

The purpose of the study is to test whether K-bentonites may contain a more complex history than previously thought. Any number of physical and biological factors could influence a volcanic ash layer during the eruption, deposition, burial, and preservation prior to exhumation. When considering the history of volcanic eruptions during the Acadian Orogeny, Devonian K-bentonites demonstrate that the beds may either (1) contain volcanic material from a single eruptive event, (2) contain material from multiple eruptive events, and the beds are expressed as multiple-layered K-bentonites, or (3) comprise a mixing of volcanic material from a couple to many ashfall events. The presence of distinctive physical features within layer samples or inconsistent elemental abundances within phenocrysts from subdivisions of the same bed could support the idea that more than one eruptive event took place. This detailed study of the sedimentology and geochemistry of certain Devonian K-bentonite layers is an attempt to better understand the history and preservation of many of these beds throughout the Appalachian Basin.

PREVIOUS WORK ON DEVONIAN K-BENTONITES

Studies regarding the geologic implications that are recorded in many Paleozoic K-bentonites and their ability to convey information about tectonic events have become more abundant (Samson et al., 1988, 1990; Delano et al., 1990; Schirnack, 1990; Ebert et al., 1992; Lindstrom et al., 1992; Waechter, 1993, Waechter et al., 1993; Brett and Ver Straeten 1994; Delano et al., 1994; Hansen, 1995; Ver Straeten, 1996, 2001, 2004; Dannenmann 1997; Huff et al., 1999; Shaw, 2001, 2003). These studies have shown that K-bentonite layers contain a significant amount of information leading to a better understanding of the tectonic setting present during their deposition and ultimate preservation.

FIELD AND LABORATORY METHODS

Physical observations have shown that many K-bentonite beds may be a combination of more than one volcanic eruption or eruptive event. In addition, geochemical investigations show that various geochemical analyses are very useful in examining the volcanogenic characteristics of the beds. In this study, I use a combination of sedimentological approaches, geochemical analyses, and statistical tests in efforts to support recent studies concerning these beds and their record of eruptive history.

In the field, K-bentonite beds are recognized by a number of key factors. First, since most beds are predominantly clay rich, they weather more quickly than the surrounding strata resulting in a notch or gap between rock layers adjacent to the volcanic beds. Second, they have a tendency to support plant life that extends

along the plane of the beds, creating a distinguishable marker that aids the geologist in locating some of these beds. In addition, in some cases authigenic minerals such as pyrite will weather and create a rust staining effect on the beds below the K-bentonite layer.

However, these layers may be difficult to recognize due to the tendency of these beds to be influenced by many physical and biological factors present in the depositional environment. The mixture of the ash with detrital background sediments may preserve the material in a more resistant form so that only microscopic or other more detailed examination would recognize the beds (Ver Straeten, 2004).

FIELD METHODS

Multiple Devonian volcanic layers were sampled from previously documented localities in New York, Pennsylvania, and Virginia (Smith and Way, 1983; Shaw et al., 1991; Hansen, 1995; Ver Straeten, 1996; Tucker et al. 1998; Ver Straeten, 2001; Ver Straeten, 2004). Field samples include indurated K-bentonite layers which have been slabbed and polished and/or thin sectioned to reveal finely detailed physical features of the bed and adjacent surfaces, e.g. various sedimentary structures, fossils, crystal zoning or layering and possible unconformable surfaces or hardgrounds adjacent to the beds. Additional clay-rich K-bentonite layers and bulk samples were collected from within quarries, along road cuts, or within other natural exposures using various methods to obtain undisturbed, uncontaminated samples. Layer samples of various clay-rich Devonian

K-bentonites were impregnated with epoxy and thin sectioned in efforts to reveal finely detailed sedimentary features found within these layers. In the laboratory, bulk K-bentonite layer samples were examined for varying phenocryst abundances reflective of multiple events contained within each K-bentonite layer. Samples were processed into clay and phenocryst fractions to obtain apatite crystals for geochemical analyses. ICP-MS (Inductively Coupled Plasma Mass Spectrometry) analysis examined elemental concentrations within the phenocrysts from individual K-bentonite beds.

ANALYTICAL METHODS

Sample Preparation

Bulk samples collected for slabbing were cut and polished using basic cutting and polishing techniques. Bulk clay layer samples of individual K-bentonite layers were sampled in efforts to examine the microscopic features visible using thin sectioning. Owing to the delicate nature of most of the K-bentonite layer samples, an independent laboratory prepared the samples.

All samples were processed for geochemical analysis using Inductively Coupled Plasma Mass Spectroscopy (ICP-MS) following similar procedures as described in Shaw (2003). Bulk K-bentonite samples of up to 20 kilograms were liquefied into clay and phenocryst size fractions using rock tumblers. The resulting mixture was wet sieved and grains smaller than or equal to 150 μ m were retained and sent through a Roger's Table to isolate grains according to individual crystal density. Lighter grains were dried and set aside for future analyses. Grains of highest density were

isolated, and then rinsed repeatedly with acetone to facilitate faster drying. Once dry, grains were separated using Acetylene Tetrabromide (CHBr_2)₂; Sp.Gr:2.97). Light separates were cleaned using acetone and stored for future analyses. After rinsing with acetone, heavy separates were dried, and then cleaned using a sonicator and Sodium Oxalate ($\text{C}_2\text{Na}_2\text{O}_4$) to remove any materials adhered to the grains.

A Franz Isodynamic magnetic separator using varying magnetic field strengths generated by indicated currents of 0.5 A, 1.0 A, and >1.5 A was used to isolate apatite from magnetic phases. Magnetic crystals were labeled and stored for future analyses. In some cases, further phenocryst separation of apatite and zircon grains using Methylene Iodide (CH_2I_2 ; Sp.Gr:3.325) was necessary. Once divided, apatite phenocrysts were hand picked under a binocular microscope.

Crystal Selection and Digestion

Table 1 lists the geographic locality and total number of apatite phenocrysts selected for analysis at each location. In order to minimize contamination, crystals that are closest to euhedral, are apparently inclusion-free, and are uncoated and relatively clean are desirable. The size of the crystals is not important, only that they fit these criteria. However, in cases where apatite abundances are low, crystals that do not fit these standards must be used due to decreased availability of the grains in order to obtain statistical information for comparison (Shaw,

Sample Locality Layer (Cluster) Name	Layer Name	Thickness (cm)	Crystals Selected (Used)	Crystal Condition
Seven Fountains, Virginia Edgecliff and Moorehouse Member Equivalents of the Onondaga Formation including Tioga Middle Coarse Zone	7 Fount 1(a)	5	20(12)	Euhedral and subhedral grains. Some clean, some dirty. Few grains. Mostly clean grains. Many euhedral grains. Clean. Abundant clear euhedral grains.
	7 Fount 1(b)	5	20(19)	
	7 Fount 1(c)	5	20(20)	
	7 Fount 3	8	20(18)	
Cobleskill, New York Sprout Brook K-bentonite Cluster Spawn Hollow Member of Esopus Formation	CL# 2	2-4	100(90)	Abundant euhedral grains. Some clean, some are dirty.
	CL# 3(a)	3	60(39)	Many large euhedral grains, some subhedral. Crystals appear dirty.
	CL# 3(b)	3	20(20)	Abundant grains. Large crystals. Crystals appear dirty.
	CL# 3(c)	3	20(19)	Few large grains. Some clean, some are dirty.
	CL# 3(d)	1	20(17)	Large crystals. Crystals appear dirty. Some clean crystals.
	CL# 3(e)	1	20(20)	Abundant large euhedral grains. Crystals appear dirty.
	CL# 3A	0.5	20(16)	Both euhedral and subhedral grains.
	CL# 4	4-6	60(56)	Few Pristine, Euhedral Grains.
Auburn, New York Tioga B K-bentonite Onondaga Formation	Oak 0-4.5	4.5	40(27)	Abundant euhedral grains. Clean.
	Oak 0-16.0	16	40(40)	Abundant euhedral grains. Clean. Large crystals.
Seneca Falls, New York Tioga B K-bentonite Onondaga Formation	SF 0-5	5	60(52)	Few quality grains, some euhedral. No visible color difference.
	SF 5-8	3	60(51)	Few grains. Subdivided based on bluish color of crystals.
	SF 5-8(Clr)	-	40(27)	Few grains. Crystals subdivided based on clear to smoky appearance.

Table 1: Table listing the condition and number of crystals selected from each geographic locality and layer in which individual apatite phenocrysts were selected for ICP-MS analysis. Values in parentheses are the number of crystals that yielded trace element data using the ICP-MS analytical method.

2003). Once the phenocrysts are chosen, individual crystals are placed into separate disposable polyethylene test tubes. Ten milliliters of 0.5% HNO₃ containing 10 ppb of Ga, Sc, Cs, In, Re, and Bi as internal standards is added to each test tube and then shaken to dissolve the apatite. The blank contains 100 milliliters of the 0.5% HNO₃ solution. The three analytical standards are mixtures of 99.9 ml of the 0.5% HNO₃ solution and 100 µL of a stock analytical solution made from the homogenized powder of a single, large apatite crystal originally in excess of 300 g. In order to obtain background concentrations of the rare earth elements representative of a typical apatite crystal, this powder is mixed into three solutions of varying concentrations. Without these three analytical standards concentrations of trace and REE from the individual apatite crystals would be below the limit of detection of

the instrument. Upon analysis the instrument will detect the background values from these pulverized crystal standards, in addition to those concentration values from the individual crystals studied.

Analytical Method

Trace element concentrations of apatite crystals are analyzed using the PerkinElmer/Sciex Elan 6100 DRC Inductively Coupled Plasma Mass Spectrometer at Union College, Schenectady, New York. Analytes include: P, Ca, Sr, Y, Rare Earth Elements (REE), Pb, Th, and U. Each individual crystal solution is analyzed sixteen times, where each of these sixteen runs contains five replicated analyses. Analyzing the crystals in this way decreases the analytical error and increases instrument precision. Data from these analyses can be found in Appendix B.

Statistical Method

Apatite phenocrysts have a high survival rate in volcanic layers and are useful tools in testing the interlayer and intralayer homogeneity. In order to obtain enough statistical data, approximately 20 apatite crystals must be selected from each layer. The current analytical method used by this investigator and Shaw (2003) analyzes trace elements from individual apatite crystals from a given layer. Phenocrysts are analyzed individually, and then the geochemical data is compared statistically to all other crystals from the same layer.

In this study, the weight of each separate crystal could not be measured. Therefore, the relative abundances of trace and REE

concentrations can be used to distinguish crystals based on the proportion of these concentrations within the crystal. Crystals from the same magma will have the same proportion or ratio of elements within them. Using the Tukey-Kramer HSD test, population means of these elemental ratios can be used to test the variability of crystal populations within a layer.

The Tukey-Kramer Honestly Significant Difference [HSD] test; (Sall et al., 2001) is designed to measure the differences displayed in the various trace element plot figures found in the text and Appendix B. Similar to Student's t-test, this statistical test compares the means of the analyte concentrations for each crystal population by using the standard error of the mean to find out whether two means are similar, indicating they originate from the same population. If a crystal is significantly different from another population, then this difference is indicated in the resulting table.

SAMPLE LOCALITIES

K-bentonites examined in this study are from Lower to Middle Devonian marine strata from outcrop, roadcut, and quarry locations throughout New York, Pennsylvania, and Virginia. These localities, labeled A-I, are shown on Figure 1. This section will include brief geographic and geologic descriptions for each sampling site. Geologic symbols for stratigraphic cross-sections, in addition to further information for all localities can be found in Appendix A. In addition, due to the theft of valuable stratigraphic information prior to the completion of this manuscript, certain stratigraphic

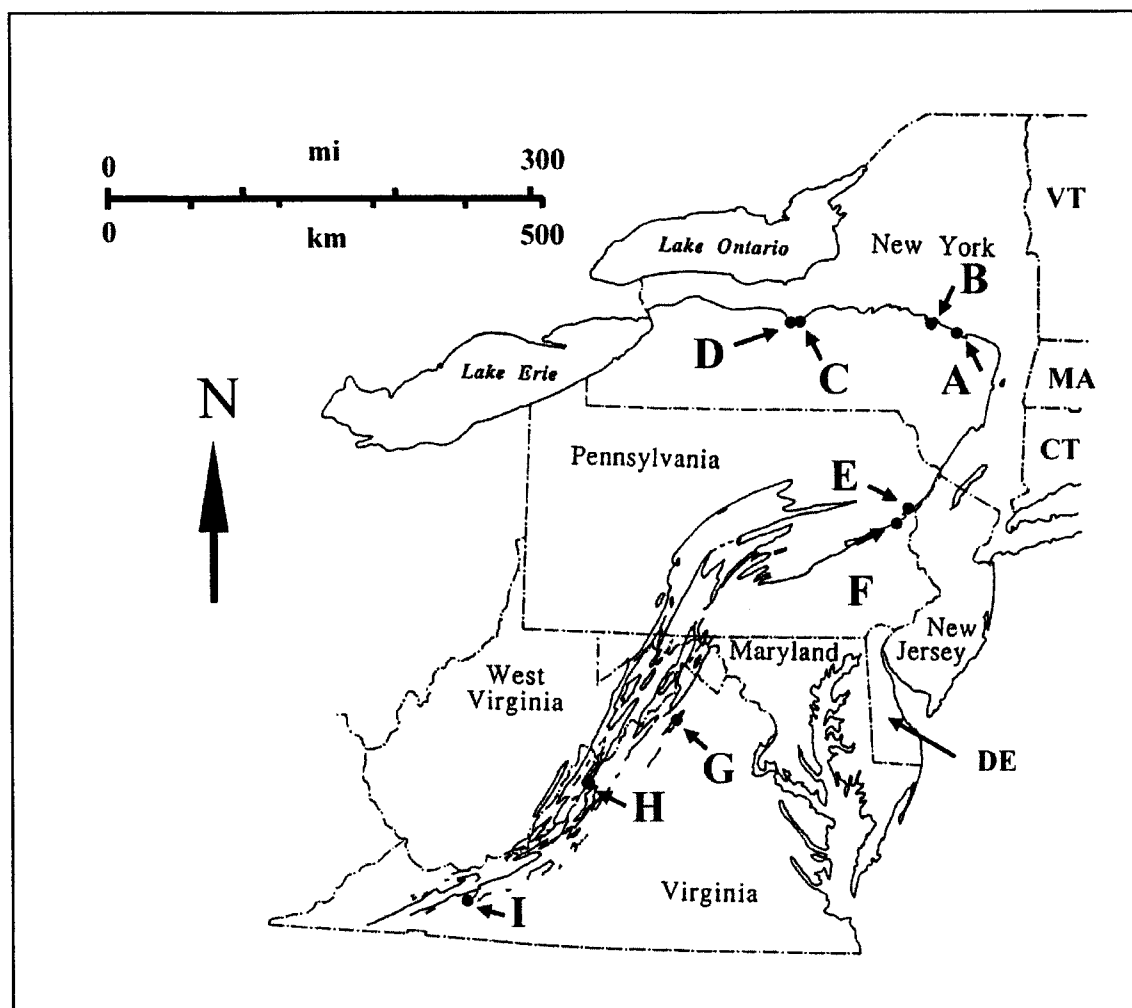


Figure 1: Map of the eastern United States showing the Devonian outcrop belt and all sampling sites utilized in this study. Locations are (A) Cobleskill, New York. (B) Cherry Valley, New York. (C) Auburn, New York. (D) Seneca Falls, New York. (E) Echo Lake, Pennsylvania. (F) Stroudsburg, Pennsylvania. (G) Seven Fountains, Virginia (Massanutten Mountain). (H) Williamsville, Virginia. (I) Wytheville, Virginia. Figure modified from Ver Straeten (1996).

sections were completed via collaboration with others, or modification from published materials (C. Ver Straeten, personal communication; Smith et al., 1988).

New York Localities

K-bentonites sampled from Locality A are from the lower Emsian Sprout Brook K-bentonite Cluster. The Cobleskill site (Locality A) is located in Schoharie County along highway cuts on south side of New York Interstate 88. The site is approximately 0.75 km east of Interstate 88 exit at New York Route 145, approximately 5.5 km east of Cobleskill, New York and contains strata of the Oriskany Formation and the Spawn Hollow and Quarry Hill Members of the Lower Esopus Formation, including the Sprout Brook K-bentonite cluster. At this site, we see alternating layers of siliceous siltstones and shales with some chert layers and K-bentonite beds. A stratigraphic section of the site can be seen in Figure 2.

The Cherry Valley locality (Locality B), located in Otsego County, contains two separate sampling sites. The first site, Cherry Valley #1, is located on the south side of US Route 20, approximately 0.4 km east of its intersection with New York Route 166, 2.5 km north-northeast of Cherry Valley, New York. Figure 3 shows a stratigraphic section of the middle part of the Kalkberg Formation, which includes Bald Hill K-bentonites A, B, and C. At this site the Bald Hill K-bentonites C was sampled.

The Cherry Valley #2 site (Locality B) is located on the north side of US Route 20, approximately 0.5 km west of its intersection

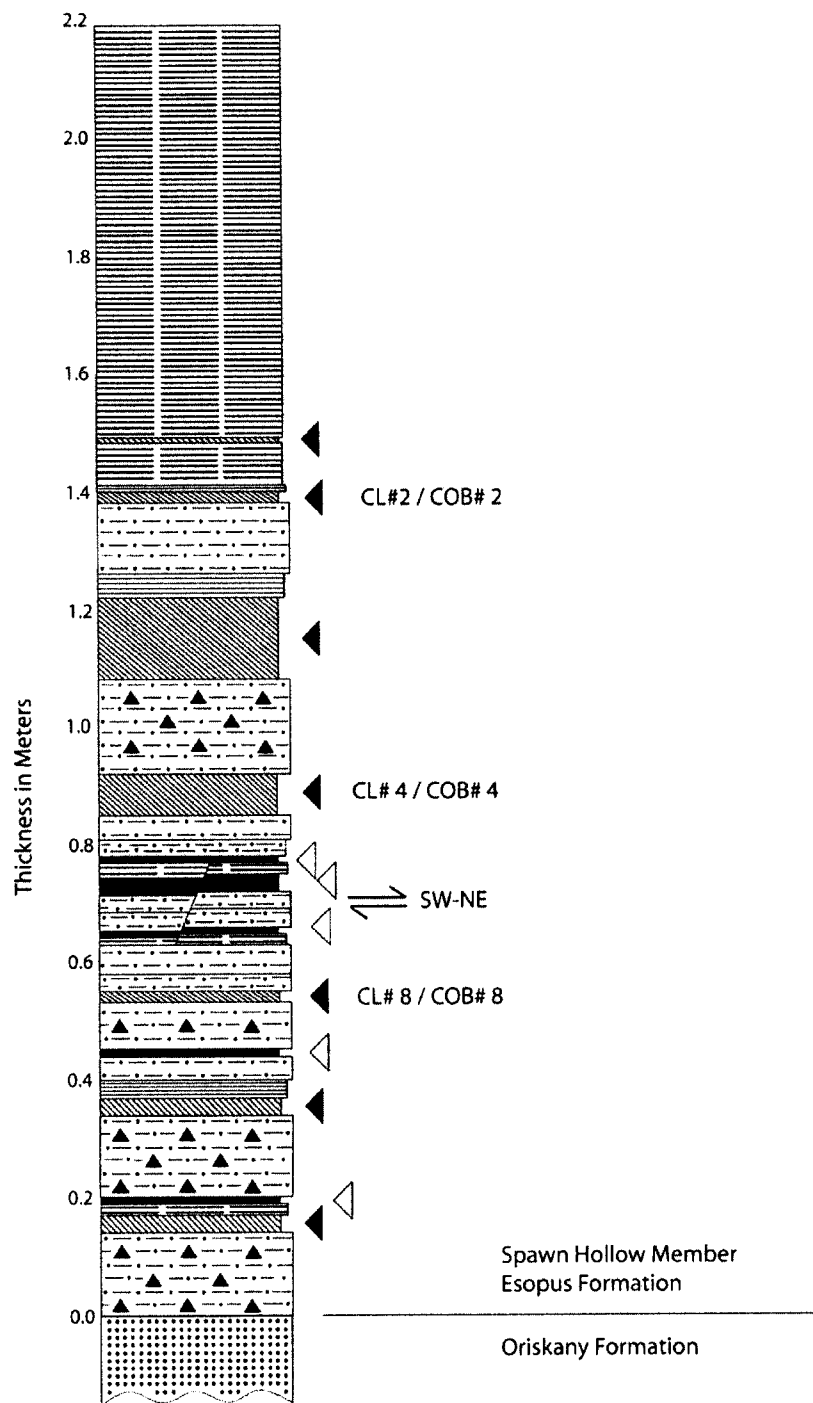


Figure 2: Stratigraphic section prepared by this investigator of geologic rock units found at the Cobleskill site (Locality A). K-bentonite layers discussed in the text are listed along with their equivalents.

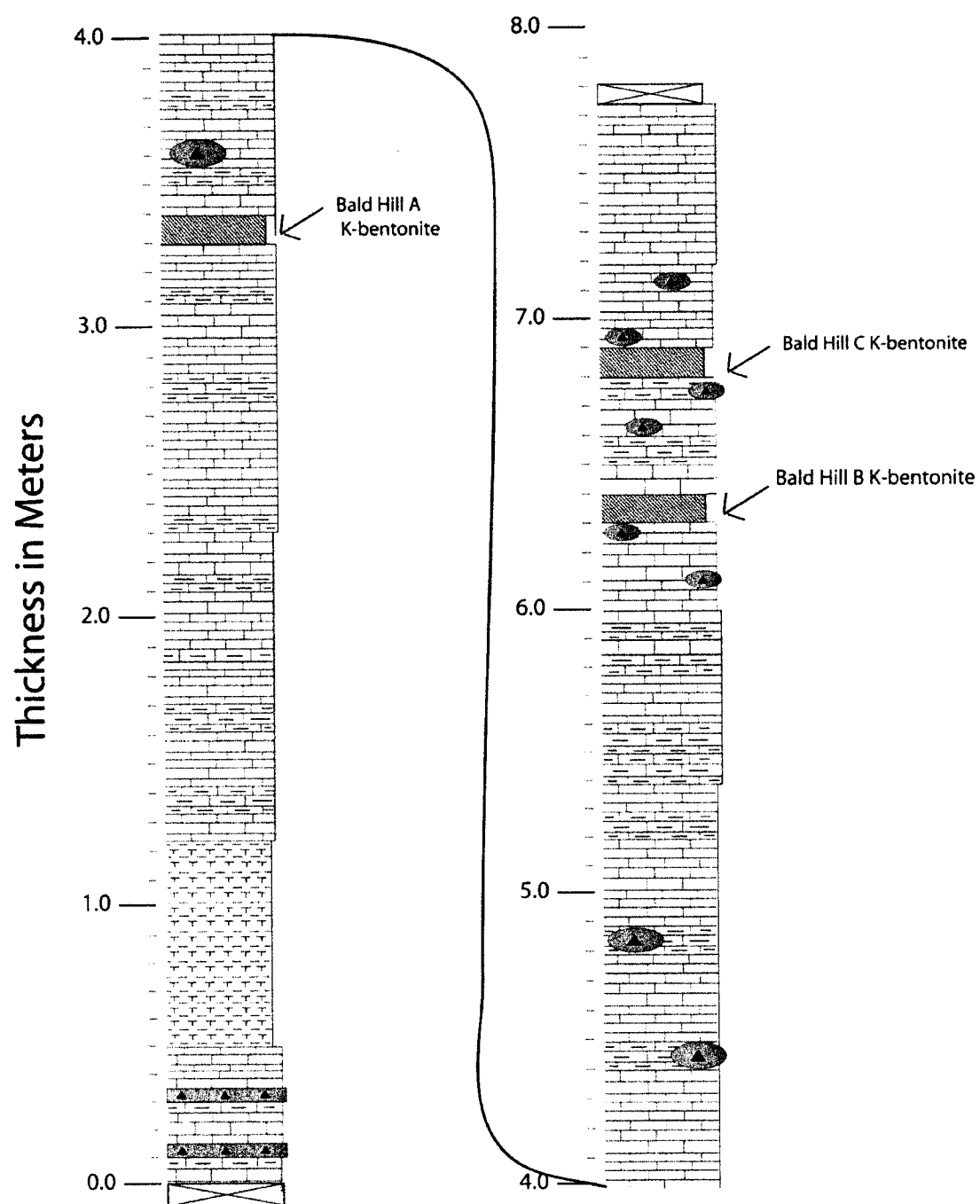


Figure 3: Stratigraphic section of the middle unit of the Kalkberg Formation at the Cherry Valley #1 site (Locality B). Modified from Smith et al., 1988.

(Figure 4) shows the Carlisle Center Member of the Schoharie Formation, and the Edgecliff Member of the Onondaga Formation. At this site a glauconitic K-bentonite layer was sampled from the formational contact between the two formations.

Both of the Cherry Valley sites contain Devonian K-bentonite beds. The stratigraphy at each locality is noted, including the positions of K-bentonite beds at each site, however, none of the K-bentonite beds were analyzed.

The Auburn site (Locality C) is located in Cayuga County within the Hansen Aggregates East Limestone Quarry, approximately 8.0 km southwest of Auburn, New York. The Tioga B K-bentonite was collected from this site. Figure 5 shows a stratigraphic section of the Auburn site containing the Moorehouse and Seneca Members of the Onondaga Formation, including the Tioga B K-bentonite at the contact between the two formations.

The Seneca Falls site (Locality D), also known to many as the Seneca Stone Quarry, is located in Seneca County within the Seneca General Crushed Stone Quarry, 5.1 km south-southeast of Seneca Falls and 1.8 km west of Canoga Springs, New York. Figure 6 shows a stratigraphic section of the Locality D containing the Moorehouse and Seneca Members of the Onondaga Formation, including the Tioga B K-bentonite.

Pennsylvania Localities

Locality E, Echo Lake, is found in Monroe County on the north side of Fairway Ridge Road at Fairway Ridge, 1.6 km northeast of Echo Lake, Pennsylvania and 1.2 km southwest of Shoemakers,

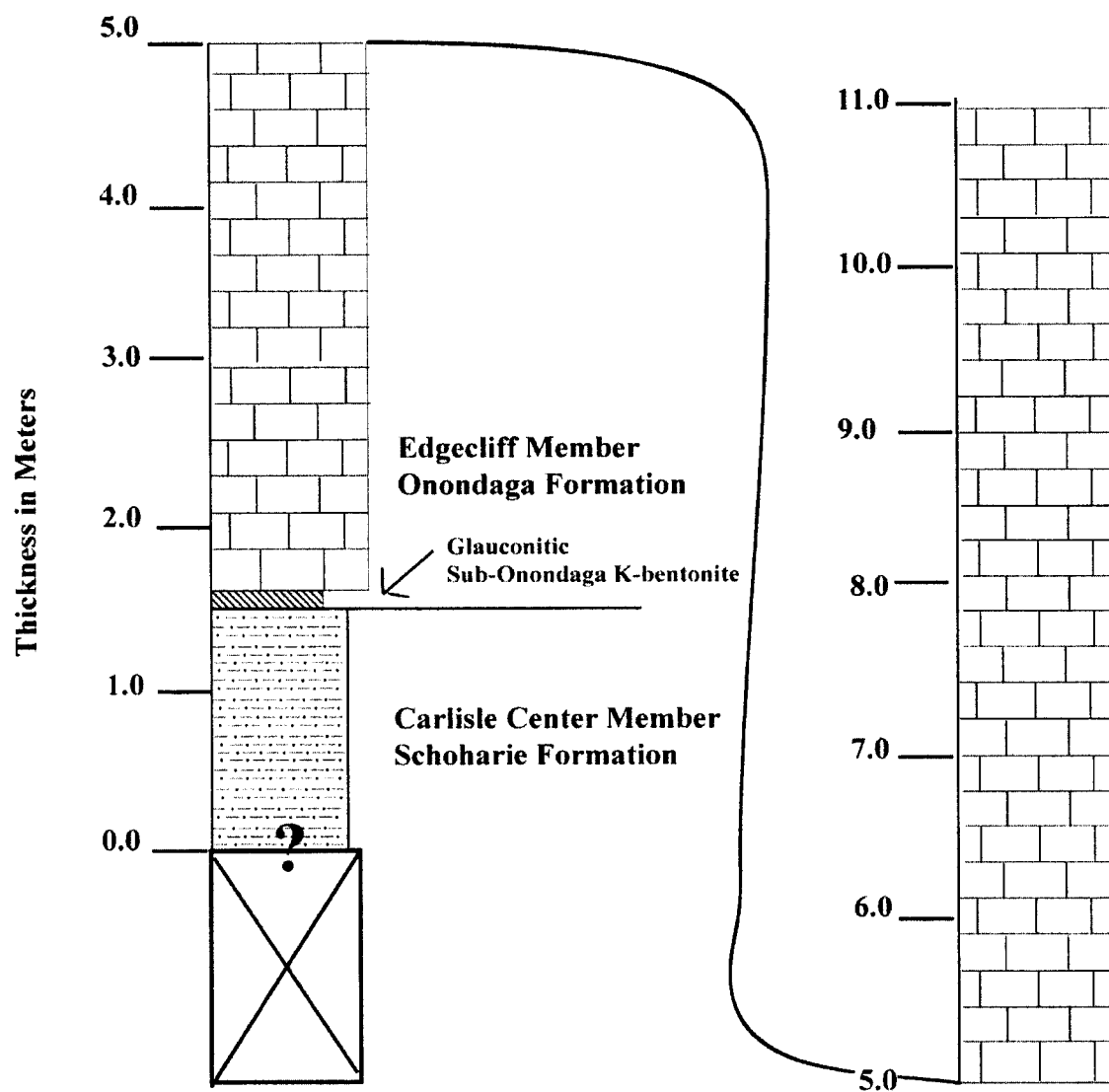


Figure 4: Stratigraphic section of geologic rock units found at the Cherry Valley #2 site (Locality B). Section prepared in collaboration with Charles A. Ver Straeten (personal communication).

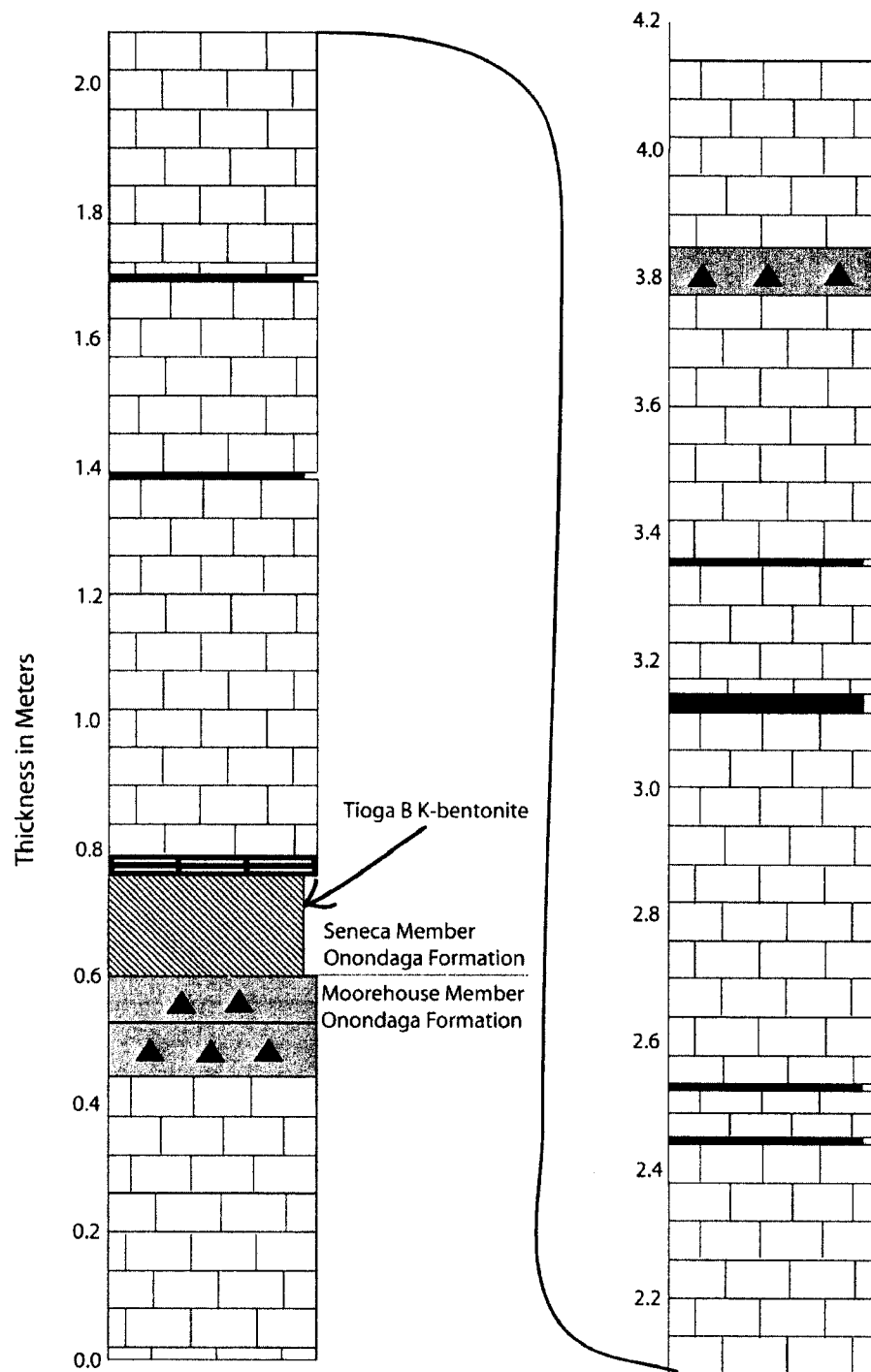


Figure 5: Stratigraphic section of rock units found at the Auburn site (Locality C) showing the Moorehouse and Seneca Members of the Onondaga Formation, in addition to the 16 cm Tioga B K-bentonite at the site.

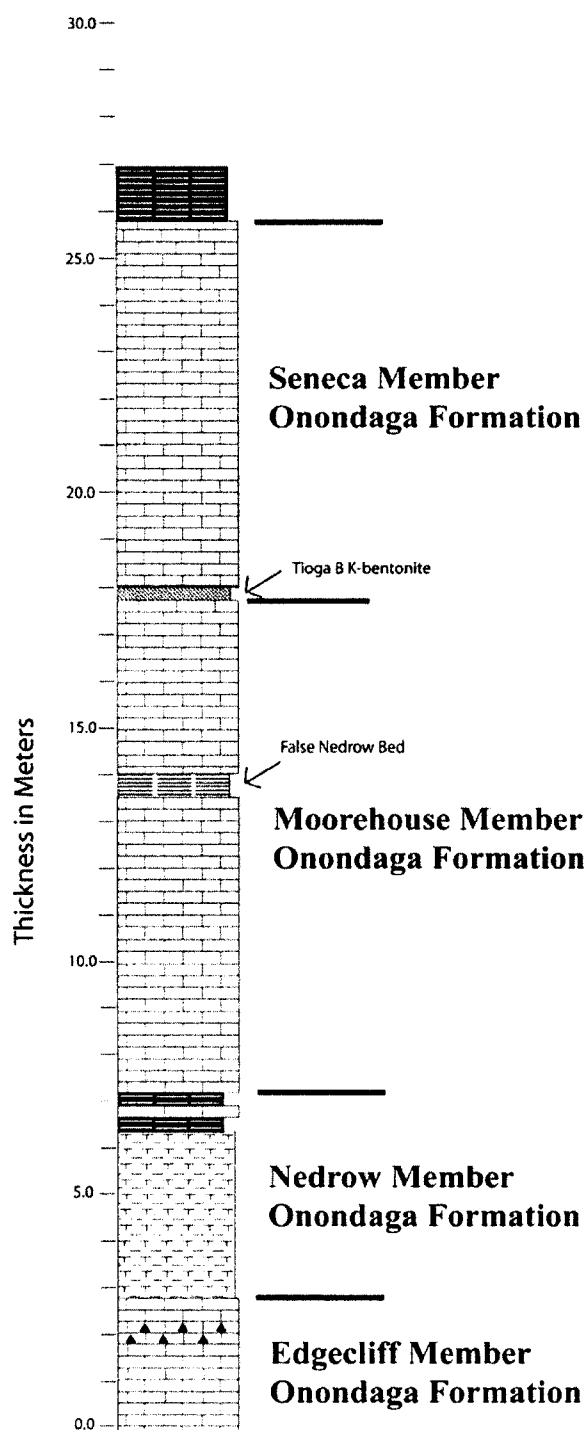


Figure 6: Stratigraphic column of rock units found at the Seneca Falls site (Locality D) showing the Moorehouse and Seneca Members of the Onondaga Formation, in addition to the 15 cm Tioga B K-bentonite at the site. Section prepared in collaboration with Charles A. Ver Straeten (personal communication)

Pennsylvania. Figure 7 shows a stratigraphic section of the Locality D containing the Moorehouse and Seneca Members of the Onondaga Formation, including the Tioga B K-bentonite. This locality is also Stop 8 in Ver Straeten et al. (2001). with New York Route 166, and approximately 2.5 km north of Cherry Valley, New York. A stratigraphic section of the site

Also located in Monroe County is the Stroudsburg site (Locality F). This site is found on the south side of Interstate 80, east of Lee Avenue at Exit 50 of said interstate in Stroudsburg, Pennsylvania. A stratigraphic section was not taken at this site, however, Figure 8 shows a stratigraphic section of a railroad cut in East Stroudsburg, less than 1 km away. This section contains the Moorehouse and Seneca Members of the Onondaga Formation, including the Tioga B K-bentonite. This section has very similar stratigraphic characteristics and can be used to depict the rocks found at Locality F.

Virginia Localities

Located in Shenandoah County, the Seven Fountains site (Locality G) is found on the east side of Virginia Route 58, 1.5 km southeast of Virginia Route 678 and approximately 12 km east-southeast of Woodstock, Virginia. The strata is within the Selinsgrove Member of the Needmore Formation; equivalent to the Edgecliff, Nedrow, and Moorehouse Members of the Onondaga Formation in New York. Figure 9 shows a stratigraphic section of the site with the location of the three K-bentonite beds sampled from this site.

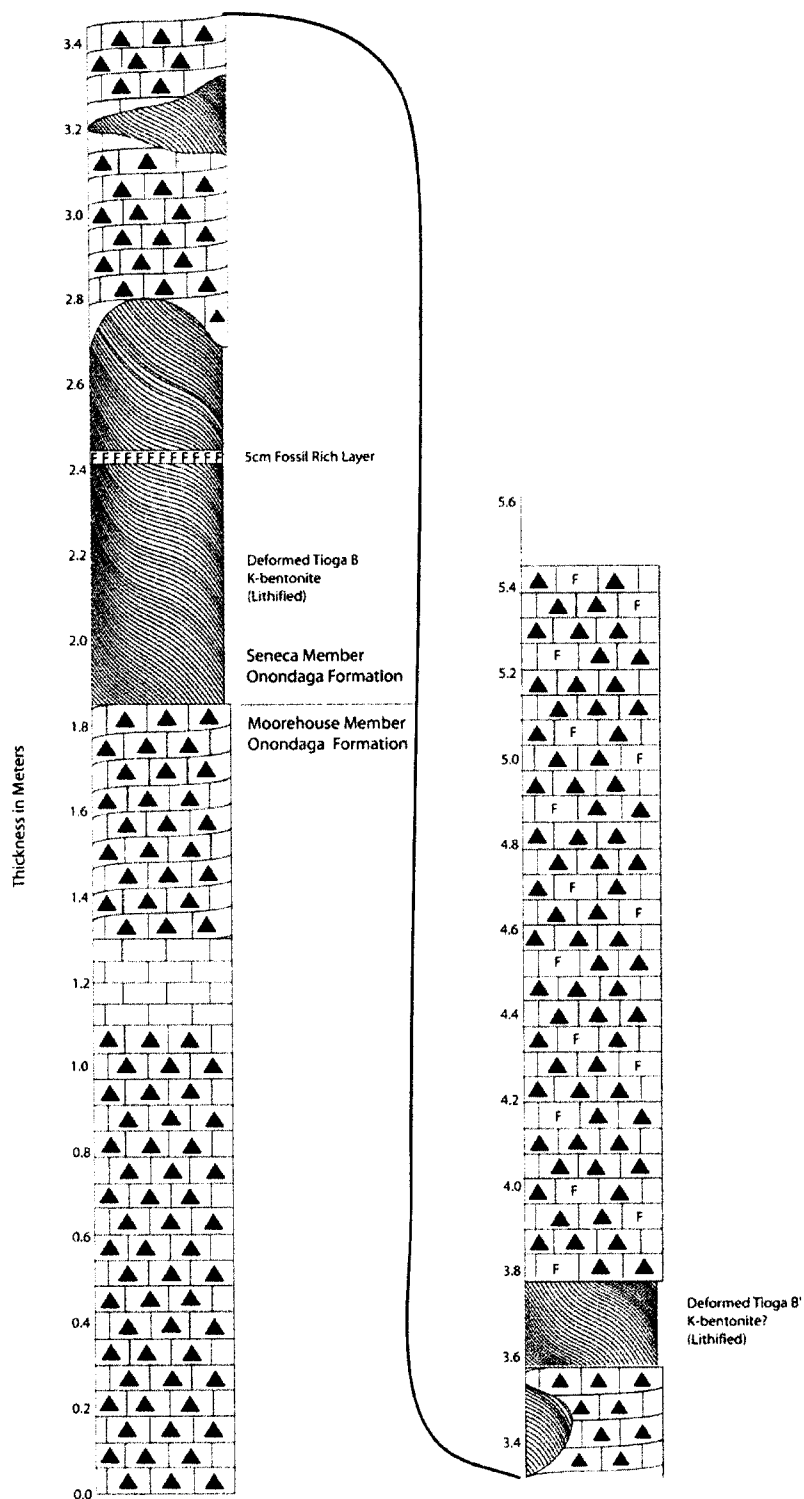


Figure 7: Stratigraphic section prepared by this investigator of geologic rock units found at the Echo Lake site (Locality E).

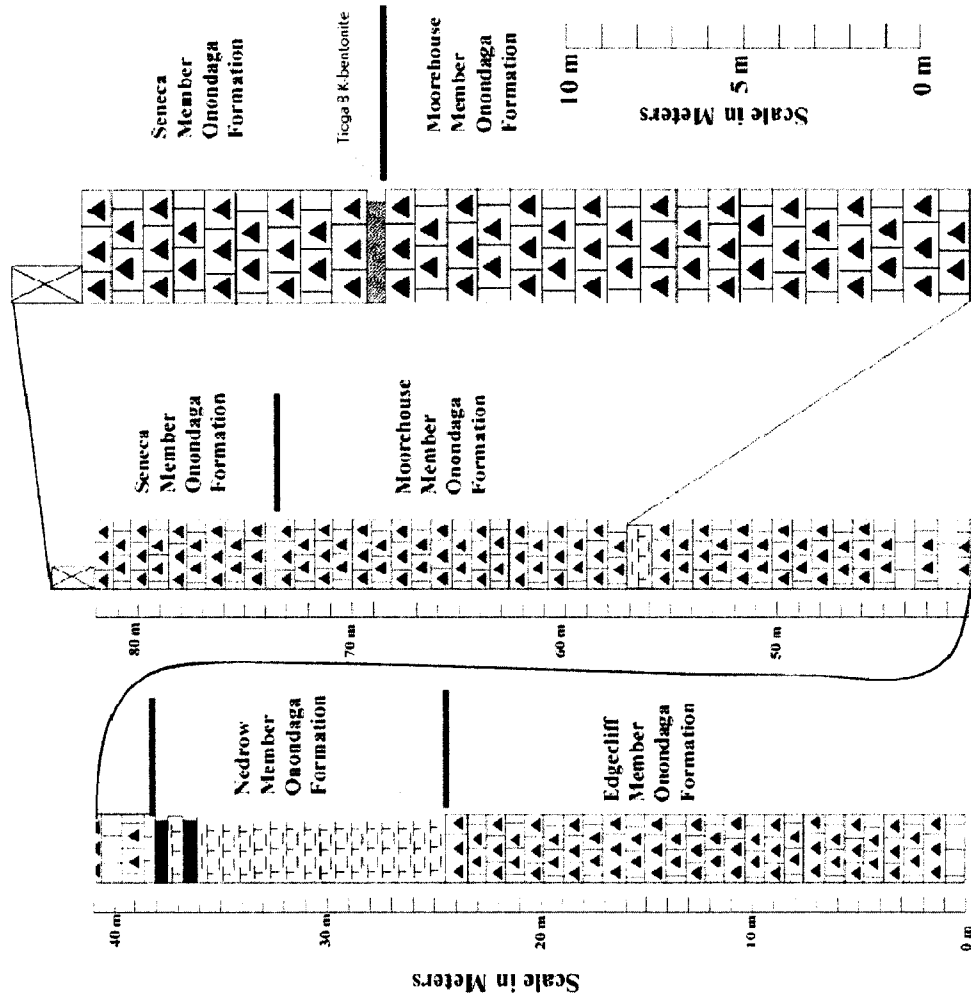


Figure 8: Stratigraphic cross-section of rock units found at a railroad cut at East Stroudsburg less than 1 km from the Stroudsburg site (Locality F) showing the Edgecliff, Moorehouse and Seneca Members of the Onondaga Formation, in addition to the Tioga B K-bentonite at the site. Section prepared in collaboration with Charles A. Ver Straeten (personal communication).

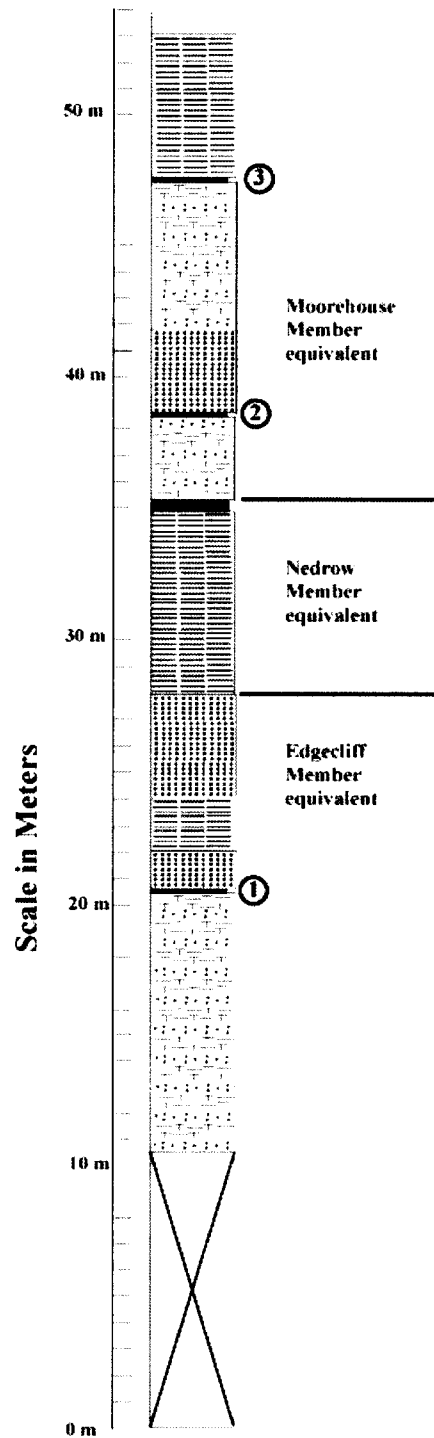


Figure 9: Stratigraphic cross-section of rock units found at the Seven Fountains site (Locality G) showing the "Selinsgrove Member" of the Needmore Formation. Numbers in yellow depict the position of the K-bentonite layers discussed in the text. Section prepared in collaboration with Charles A. Ver Straeten (stratigraphy of C. Ver Straeten).

Found in Bath County, the Williamsville site (Locality H) is located on the west side of Virginia Route 278, 3.2 km south of Williamsville, Virginia. Figure 10 displays a stratigraphic section of the site showing the Needmore Formation, including the Tioga Middle Coarse Zone. These rocks are within strata equivalent to the Edgecliff, Nedrow and Moorehouse Members of the Onondaga Formation in New York.

The Wytheville site (Locality I) is located in Wythe County along a roadcut on east side of VA Route 803, approximately 5.0 km north of Wytheville, VA. Figure 11 show a stratigraphic section of the site showing the Huntersville and Marcellus Formations, including Tioga Middle Coarse Zone. These rocks are within strata equivalent to the Schoharie and Onondaga Formations of New York.

RESULTS

This section documents both physical and geochemical evidence seen from samples analyzed in this study. Different physical/sedimentological evidence includes variations in bedding, fossils, and phenocryst layering seen both in the field and in thin section. Geochemical and statistical results are based on trace and REE concentrations for apatite phenocrysts selected from various layers. Various outcrop locations from this study contain layers that exhibit single and/or multiple lines of evidence supporting the complexity of these beds.

OBSERVABLE PHYSICAL EVIDENCE

Field Observations

Physical observations gathered while collecting samples of the

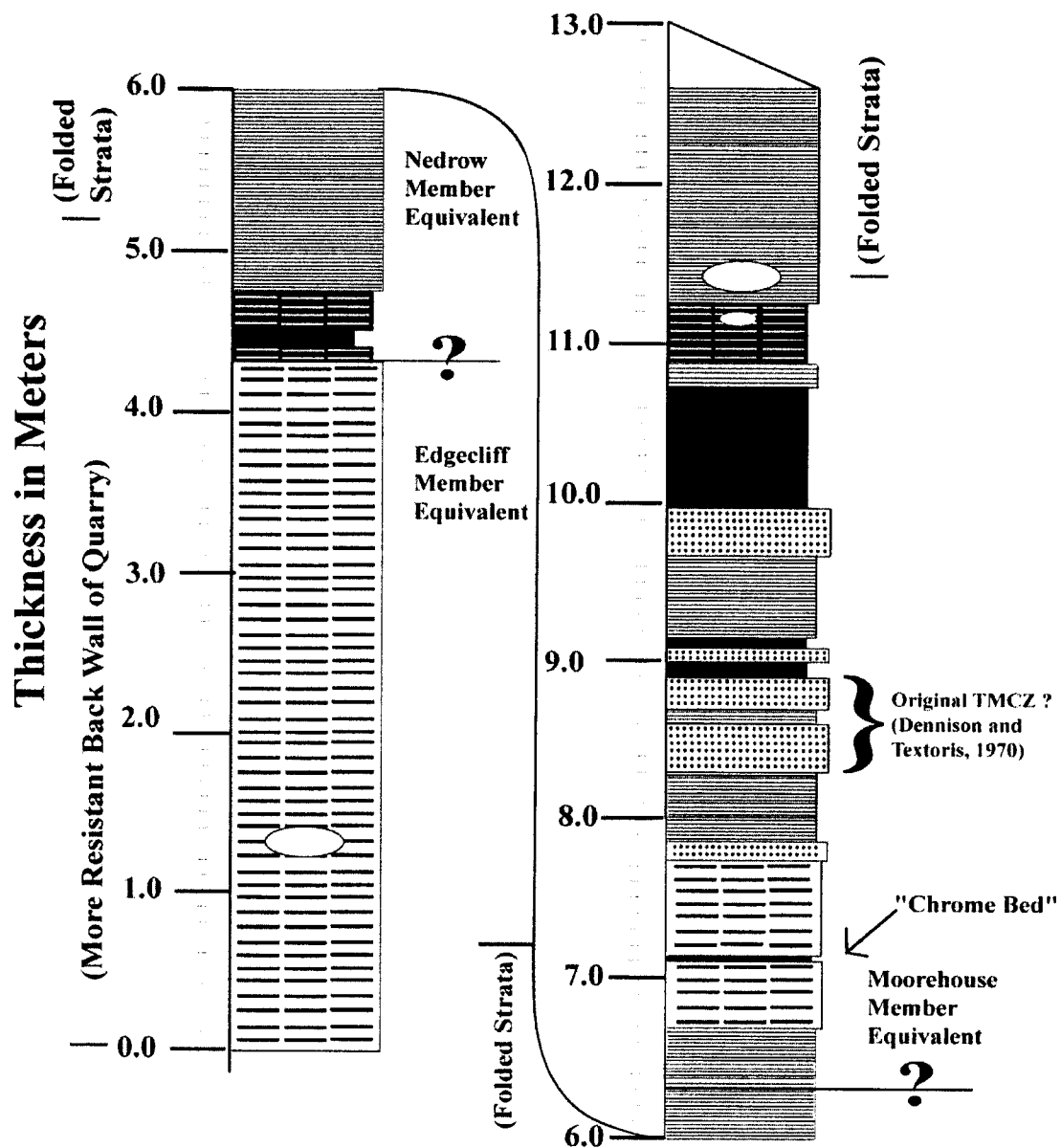


Figure 10: Stratigraphic section of rock units found at the Williamsville site (Locality H) showing the strata of the Selinsgrove Member of the Needmore Formation. Section prepared in collaboration with Charles A. Ver Straeten (personal communication).

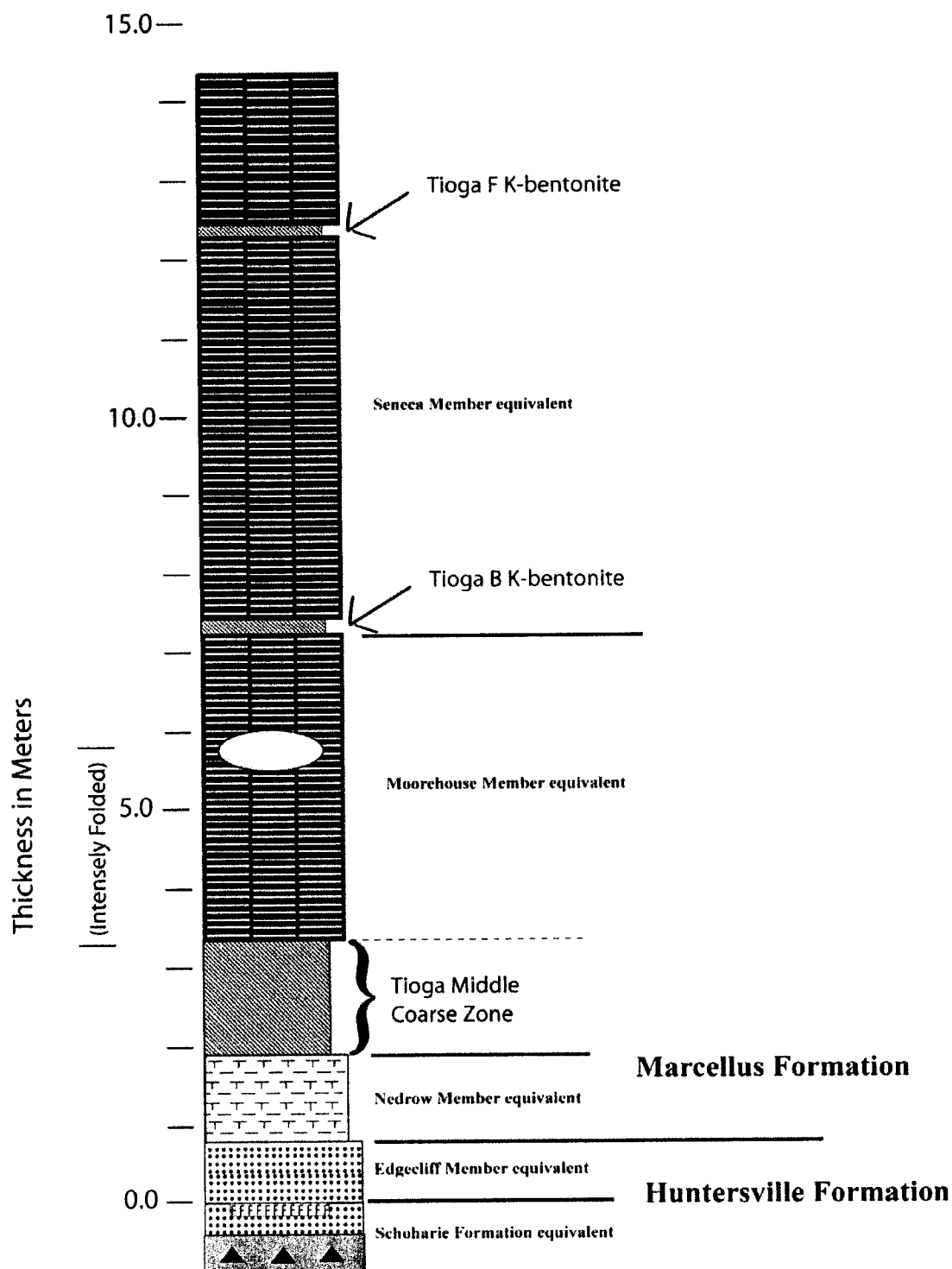


Figure 11: Stratigraphic section of rock units found at the Wytheville site (Locality I) showing the strata of the Huntersville and Marcellus Formations. Section prepared in collaboration with Charles A. Ver Straeten (personal communication).

K-bentonite beds are a type of data used in this study. This section includes physical observations seen in the field that are readily recognizable to the naked eye or with slight magnification. More detailed and microscopic features are discussed later in the section.

Examinations focused on the physical appearances of Devonian K-bentonites in the field reveal subtle variations within certain beds. One example is from an early Eifelian tuffaceous sandstone bed, 7 Fount 2, found within the Needmore Formation at the Seven Fountains site (Locality G) in northern Virginia (Figure 12). This bed does not show discrete horizontal laminae. The bed shows subtle wavy and undulating layering of the coarsely grained micas phenocrysts that make up the K-bentonite. Thin lenses of fine-grained material appear through the middle to upper portions of the bed alternating with the coarse-grained mica rich laminae. In addition, the grain size of the 7 Fount 2 bed at the Seven Fountains site is much coarser than the other beds in this study, possibly due to the proximity of the source volcano in relation to the site (Fischer and Schminke, 1984; Königer and Stollhofen, 2001). Also found at the Seven Fountains site is a 15 cm layer of volcanic origin that was subdivided into three separate five-centimeter layers based on varying physical features. These subdivisions are referred to as 7 Fount 1, with subdivisions 1a-1c where 7 Fount 1(a) is stratigraphically lower than 7 Fount 1(c). A slab sample of this bed was not obtained in its entirety, but Figure 13 shows a schematic representation of the bed based on the varying physical

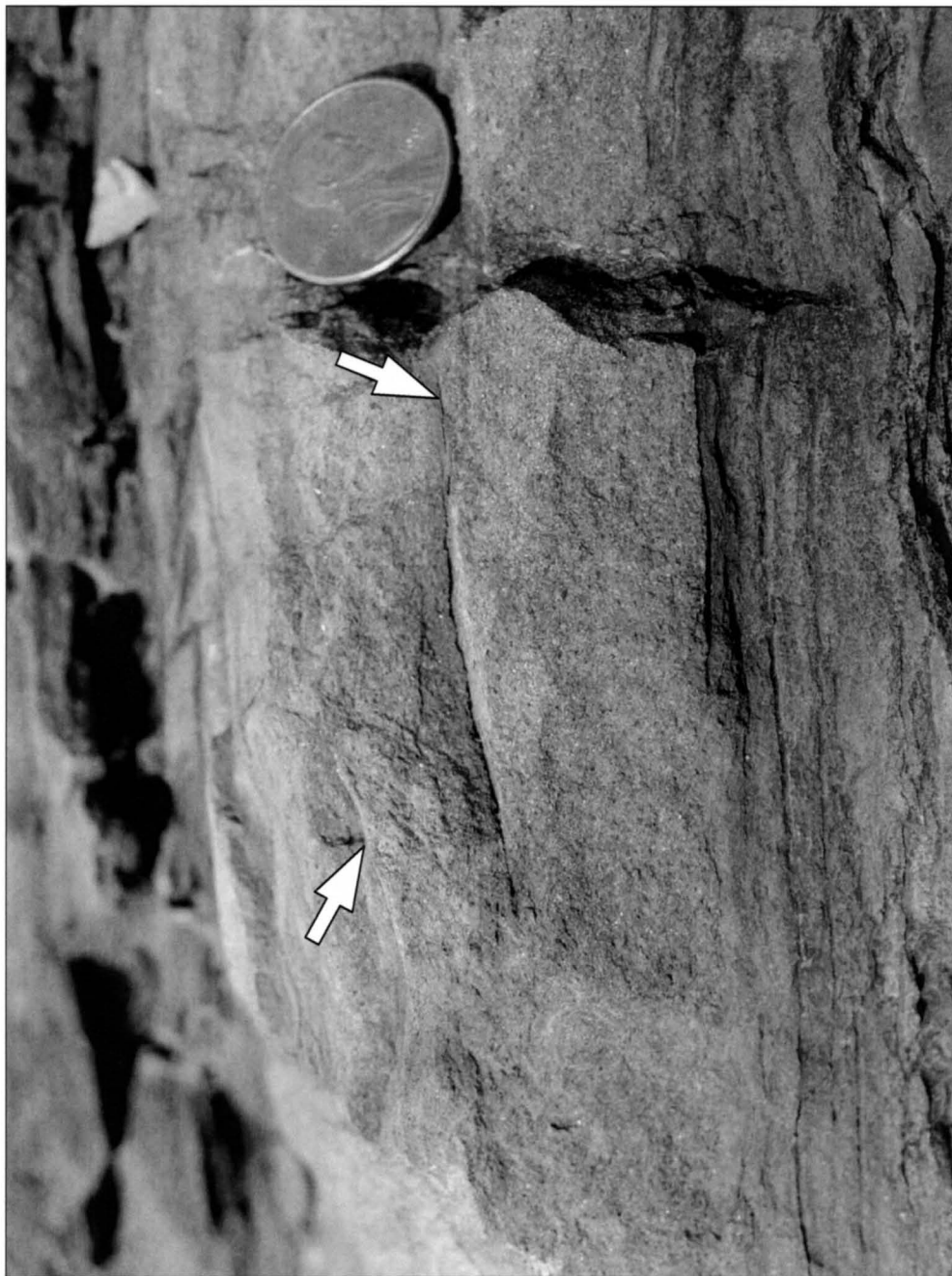


Figure 12: Sample of the tuffaceous sandstone bed 7 Fount 2 from Locality G near Seven Fountains, Virginia showing variations in bedding of the coarse, mica rich layer. Arrows point to small lenses of finer grained material. Penny provided for scale.

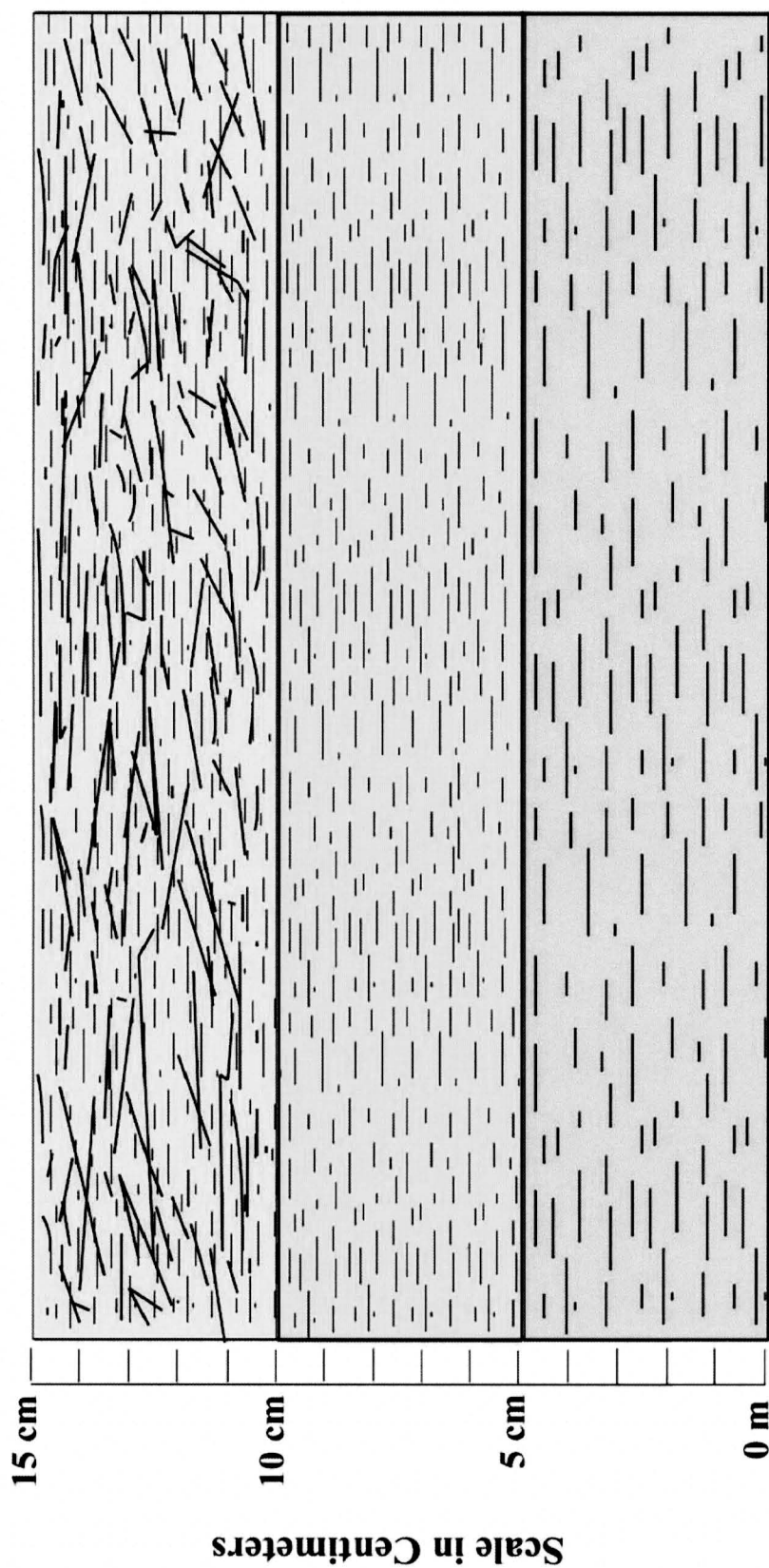


Figure 13: A schematic representation of the physical variations between the three subdivisions of 7 Fount 1 at the Seven Fountains site (Locality G). Hashed lines indicate claystone lithology. The size of the lines indicates the apparent grain size within the layer. The upper 5 cm subdivision has dark lines indicating abundant, large mica grains within the layer. Scale is provided.

characteristics. Also, Figure 14 shows a small-scale representation of the bed from small pieces of each layer to show the actual appearance of the layers relative to one another. These samples are from the litho-stratigraphic equivalent to the upper part of the Edgecliff Member of the Onondaga Formation (C. Ver Straeten, personal communication). Upon closer examination, these three layers show somewhat different physical characteristics. 7 Fount 1(a) and 7 Fount 1(b) have varying grain sizes that show a typical fining upwards trend where 7 Fount 1(b) shows the finest grain sizes of the three subdivisions, while the bottom layer, 7 Fount 1(a), shows a coarser grained texture when compared to 7 Fount 1(b). However, the upper 5 cm of the bed, 7 Fount 1(c), shows evidence of an apparent coarsening upward trend of grains size where the coarsest, micaceous grains are found in the top of the bed rather than the bottom, inconsistent with the fining upwards of 7 Fount (a) and 7 Fount (b).

Fossil Layers

The Echo Lake site (Locality E) contains a highly deformed, indurated example of the Tioga B K-bentonite found between alternating impure and slightly deformed cherty and fossiliferous limestones of the Onondaga Formation (Ver Straeten, personal communication). This layer shows significant soft sediment deformation indicated by ball and pillow structures in the bed. Within the upper third of the Tioga B at this location, a 5 cm fossil layer containing abundant brachiopod fossils *Hallinetes halli*

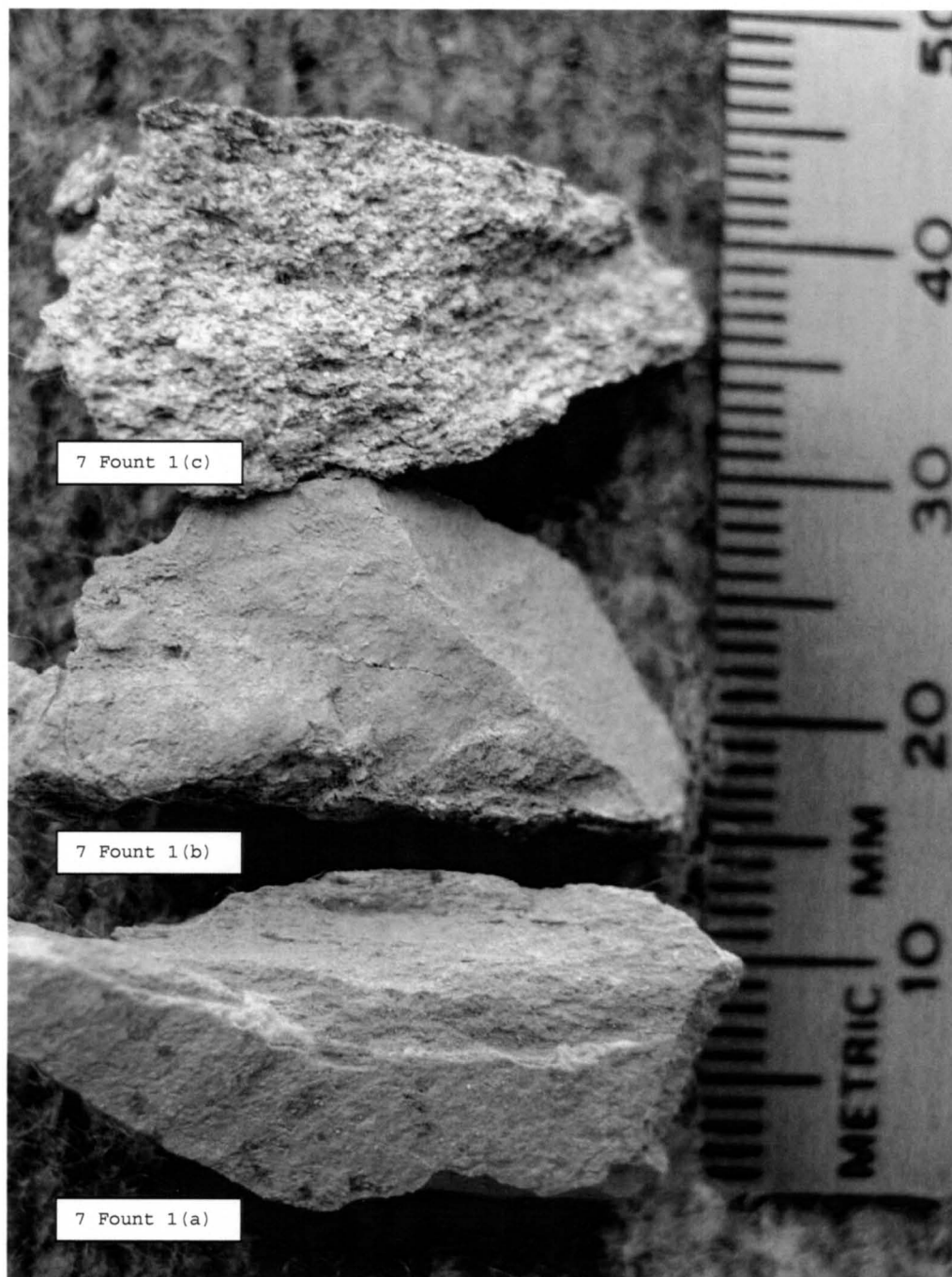


Figure 14: Small samples of the three-layered K-bentonite bed 7 Fount 1 from the Seven Fountains site (Locality G). Each piece represents a separate subdivision of 7 Fount and is labeled at the bottom left of each subdivision. Notice the coarser grained material is in the upper section of the bed. Ruler provided for scale.

is found (Figure 15). Additional information about this site can be found in Appendix A.

The Tioga B K-bentonite from Stroudsburg, PA (Locality F) also contains fossils of *Hallinetes halli* when examined with the naked eye and with a hand lens. Similar to the Echo Lake site, this site also features an indurated Tioga B K-bentonite; however, at this locality the layer shows no evidence of soft sediment deformation. The Tioga B from this site was slabbed and polished in efforts to reveal the finely detailed structures not apparent in the field. After polishing the slab, brachiopod fossils became apparent scattered intermittently through the upper 25 cm of the sample.

Physical variations in the color and apparent grain size of the Tioga B K-bentonite from Stroudsburg (Locality F) also can be seen. In the approximately 50 cm thick section of the Tioga B slabbed and polished for closer examination, a distinct color change is seen between the upper 25 cm and the lower 25 cm.

The upper portion of the slabbed sample has a dark gray to black color with a finer grained, slightly calcareous cemented matrix. In this upper portion there are abundant small-scale sedimentary features including trace fossils of burrowing organisms. In addition, there are sporadic *Hallinetes halli* brachiopod fossils found scattered throughout the upper half of the sample.

The lower half of the slabbed Tioga B K-bentonite sample from the Echo Lake site (Locality E) contains a much lighter, gray to blue gray color with coarse-grained texture and no reaction to dilute acid. No observable fossils or sedimentary structures are



Figure 15: Close up photograph of *Hallinetes halli* brachiopod fossils within the 80 cm thick deformed and lithified Tioga B K-bentonite at Locality E. Penny provided for scale.

apparent in the lower 25 cm except at the transition between the upper and lower halves where the color begins to change and fossils become apparent.

THIN SECTION ANALYSES

Figure 16 shows how thin sections can be helpful when examining the detailed fabric of a K-bentonite bed. The Tioga B K-bentonite bed from Stroudsburg, PA (Locality F) was cut into a vertical succession of 11 separate chips for thin section analysis starting at the bottom of the Tioga B K-bentonite and moving upwards. Examination of this layer in slabbed sections shows varying physical characteristics, as mentioned above. Thin sections of this layer corroborate that the bed could be subdivided into two sections based on the physical makeup of the bed.

The lower portion of the layer is coarse-grained with abundant, large biotite grains in a lighter matrix. These biotite grains are stacked on top of one another parallel to the bedding. Thin sections of this portion of the slab do not show any apparent fossils or sedimentary structures, consistent with slab evidence described above.

Moving up from the bottom of the bed toward the top, there are a number of physical differences seen within the thin sections that cannot be seen in the slabbed samples. First, the color and grain size of the matrix changes from the coarse-grained, mica-dominated lower portion of the layer, to a finer grained matrix with very few biotite grains present. Also, those few biotite grains present do not exhibit the same preferred orientation as those in the bottom of

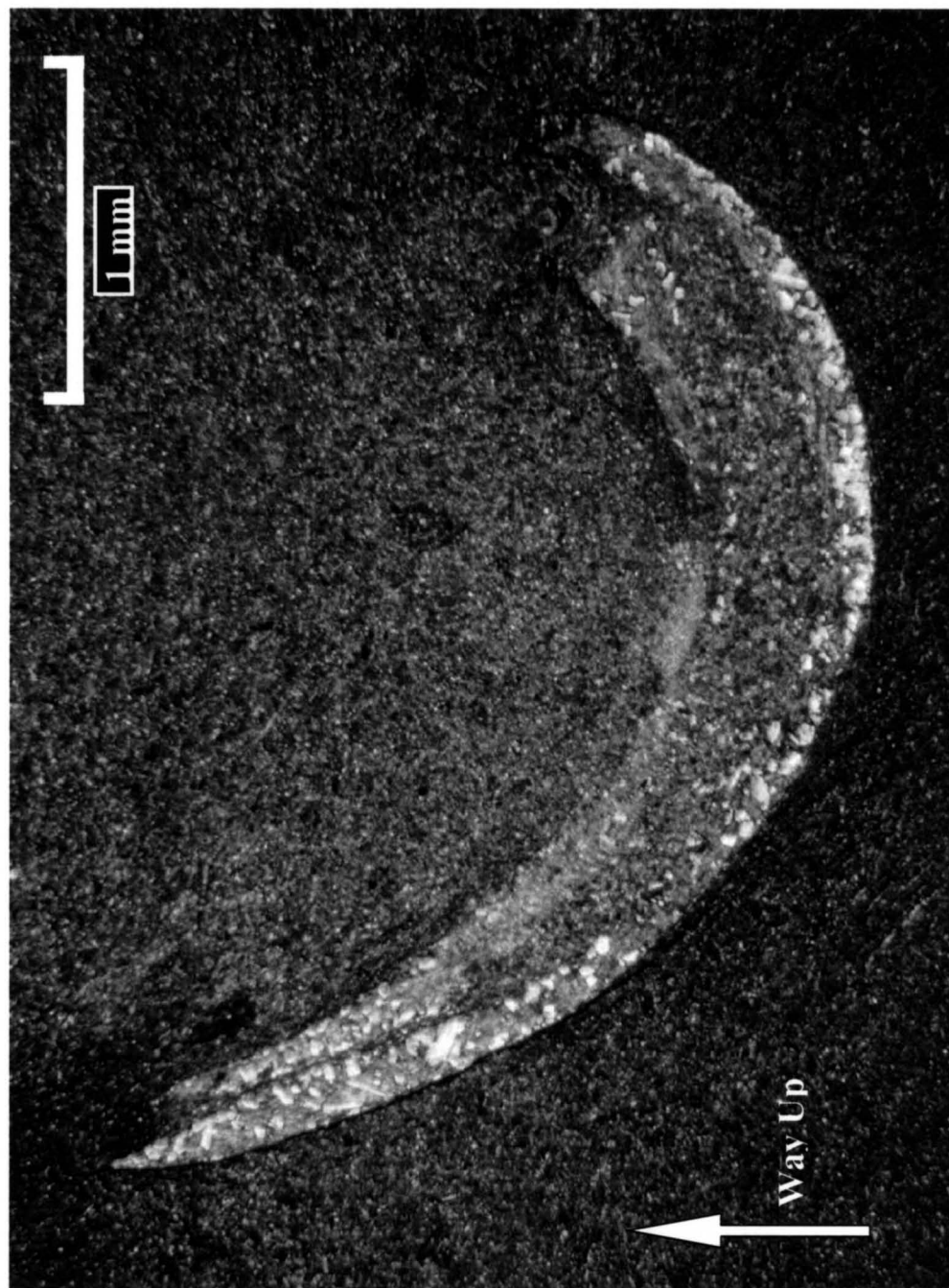


Figure 16: Photomicrograph of the Tioga B K-bentonite at Locality F showing an articulated chonetid brachiopod (*Hallinetes halli*) within the layer. Arrow indicates that the sample is oriented top up as found in the field. Scale is provided.

the section, but are scattered sparsely through this portion of the bed with no discernable preferred orientation. There are trace fossils of burrows within the top 5cm of the lower portion showing evidence of biological disruption of the soft sediment prior to burial. Lastly, as stated in a previous section, thin sections from the upper 25 cm, show scattered brachiopod fossils throughout the upper portion that are not seen in the lower portion.

Another layer that shows mineralogical variations revealed by thin section analysis is the layer referred to as the "Chrome Bed" from the Williamsville site (Locality H) (C. Ver Straeten, personal communication). Within this bed are two approximately 1 cm thick layers of coarse muscovite grains that are distinctly different, in both color and relative orientation, from the surrounding material in the layer. Figure 17 shows a portion of these muscovite-rich layers within the K-bentonite bed. The muscovite-rich layer in the upper portion of the slide shows predominantly compact, flat-lying muscovite grains with few other volcanic grains surrounding them. Conversely, the lower portion of the slide has mineralogy far lighter in color, with less abundant muscovite grains present. In addition, the lower part of the slide shows that these less abundant muscovite grains show less of a preferred orientation than the upper part of the slide. Lastly, in the center of the slide there is a band of apparent hydroxide minerals that may represent a boundary between the upper and lower sections of the bed.

7 Fount 2 from the Seven Fountains site (Locality G) also shows microscopic features. Figure 18 shows what could be subtle,



Figure 17: Photomicrograph of the "Chrome Bed" from Williamsville, Virginia (Locality H). Yellow brackets show the division of the thin section into the upper portion (C), layer of hydroxide minerals (B), and the lower portion (A). Scale is provided

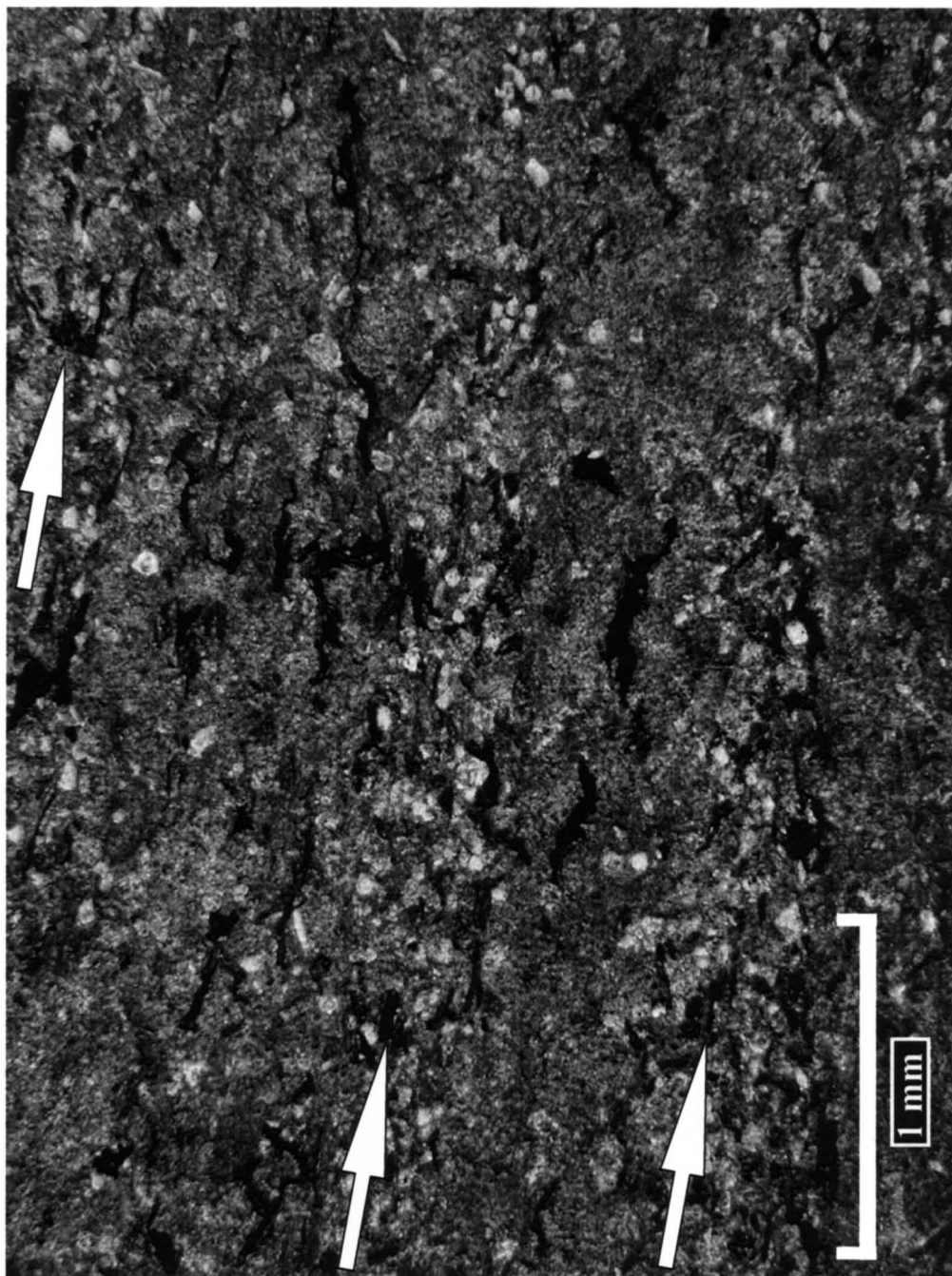


Figure 18: Photomicrograph showing a portion of 7 Fount 2 from the Seven Fountains, Virginia site (Locality G). Arrows indicate the extent and orientation of possible, subtle phenocryst layers within the K-bentonite. Scale is provided.

multiple phenocryst layers within the bed. Also, within in this bed there are burrows, seen in the slides, that indicate the activity of organisms after deposition.

GEOCHEMICAL EVIDENCE

Trace element data were obtained from Localities A, C, D, and G. Using techniques similar to those described in Shaw (2003), elemental concentrations are used to show how individual crystals from the same layer, or the same locality, plot relative to one another. These localities are described individually below.

Among the K-bentonite layers at Locality A, layers CL# 2, CL# 4, and CL# 8 have been examined most extensively with the ICP-MS analytical method. Crystals analyzed from Locality A are labeled using the acronym CL, for Cobleskill Layer. Additional samples from the Cobleskill site, labeled COB, were analyzed at Union College in Schenectady, New York by Dr. George H. Shaw (personal communication) and were sampled from the same K-bentonite beds at the Cobleskill site as the CL samples. The COB samples were collected several years prior to this study and data from these samples are used to support the precision of ICP-MS analyses and for augmentation of the data from the CL samples.

Figures 19 through 22 show the geochemical ratio plots for layers CL# 2, CL# 4, and CL# 8 respectively. The data in Figure 19 shows that samples CL# 2 and COB# 2, from the same bed, each have two distinct, closely spaced crystal populations based on the geochemistry of individual apatite phenocrysts. The two sample sites each have populations of crystals that are nearly identical.

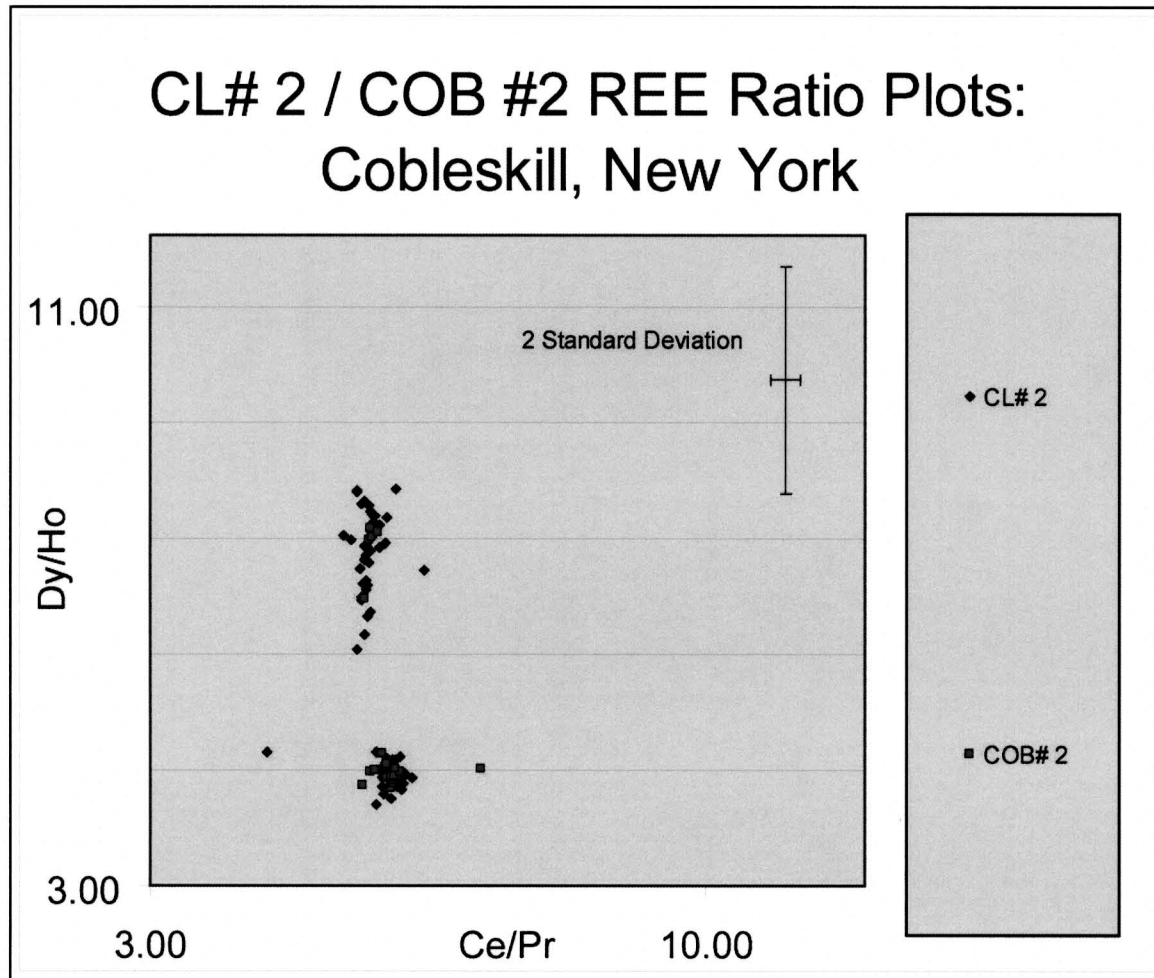


Figure 19: Rare earth element ratio plot from individual apatite phenocrysts obtained from the Esopus Sprout Brook K-bentonite layer CL# 2 at Locality A. Ratio plots from layer CL# 2 are from this study. Layer COB# 2 and corresponding plots are from the same volcanic layer. The crystals labeled COB#2 were collected in 1994 by Charles A. Ver Straeten from the same outcrop location, (but from a trench directly adjacent to the one in this study) and analyzed separately by Dr. George H. Shaw at Union College.

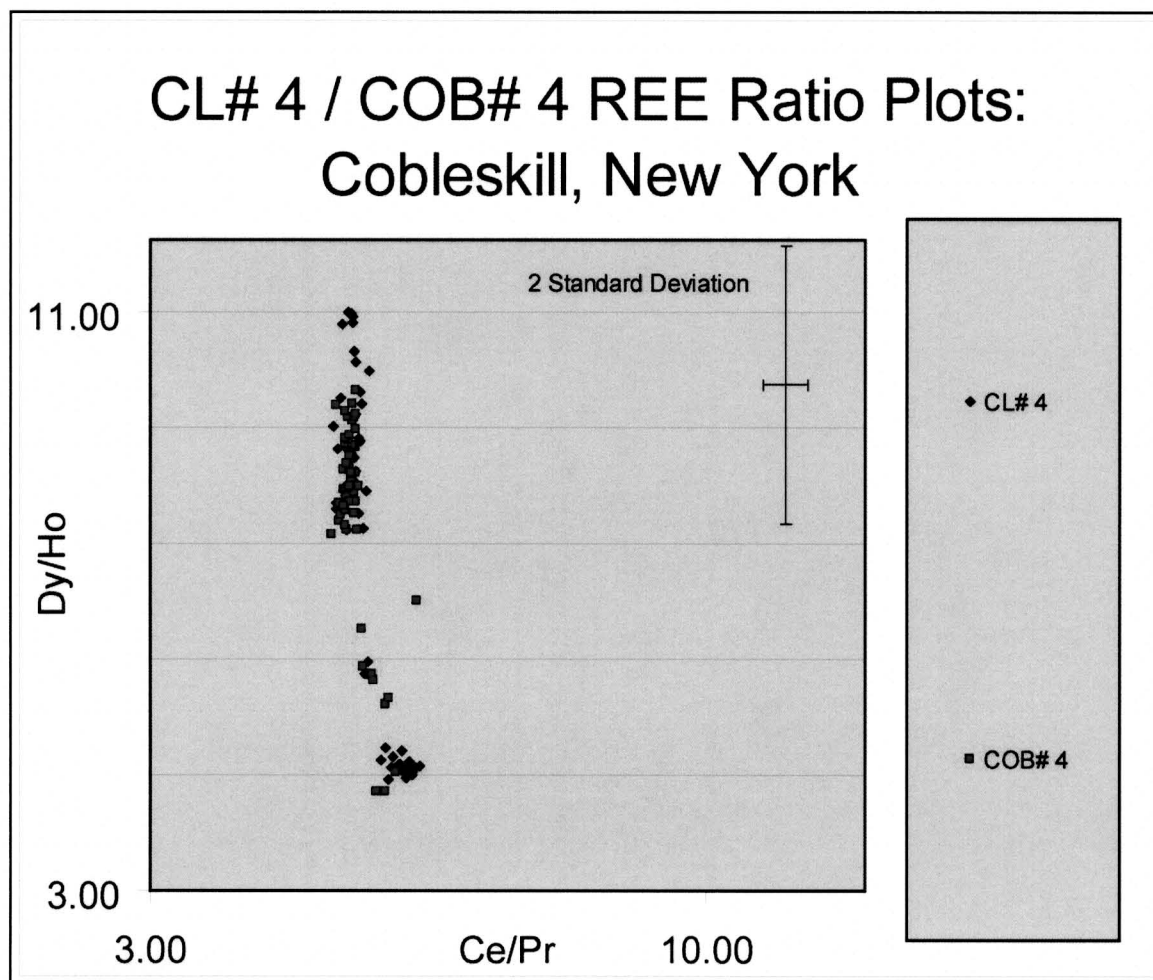


Figure 20: Rare earth element ratio plot from individual apatite phenocrysts obtained from the Esopus Sprout Brook K-bentonite layer CL# 4 at Locality A. Ratio plots from layer CL# 4 are from this study. Layer COB# 4 and corresponding plots are from the same volcanic layer. The crystals labeled COB#4 were from the same outcrop location, but from a trench directly adjacent to the one in this study and run separately by Dr. George H. Shaw for data corroboration.

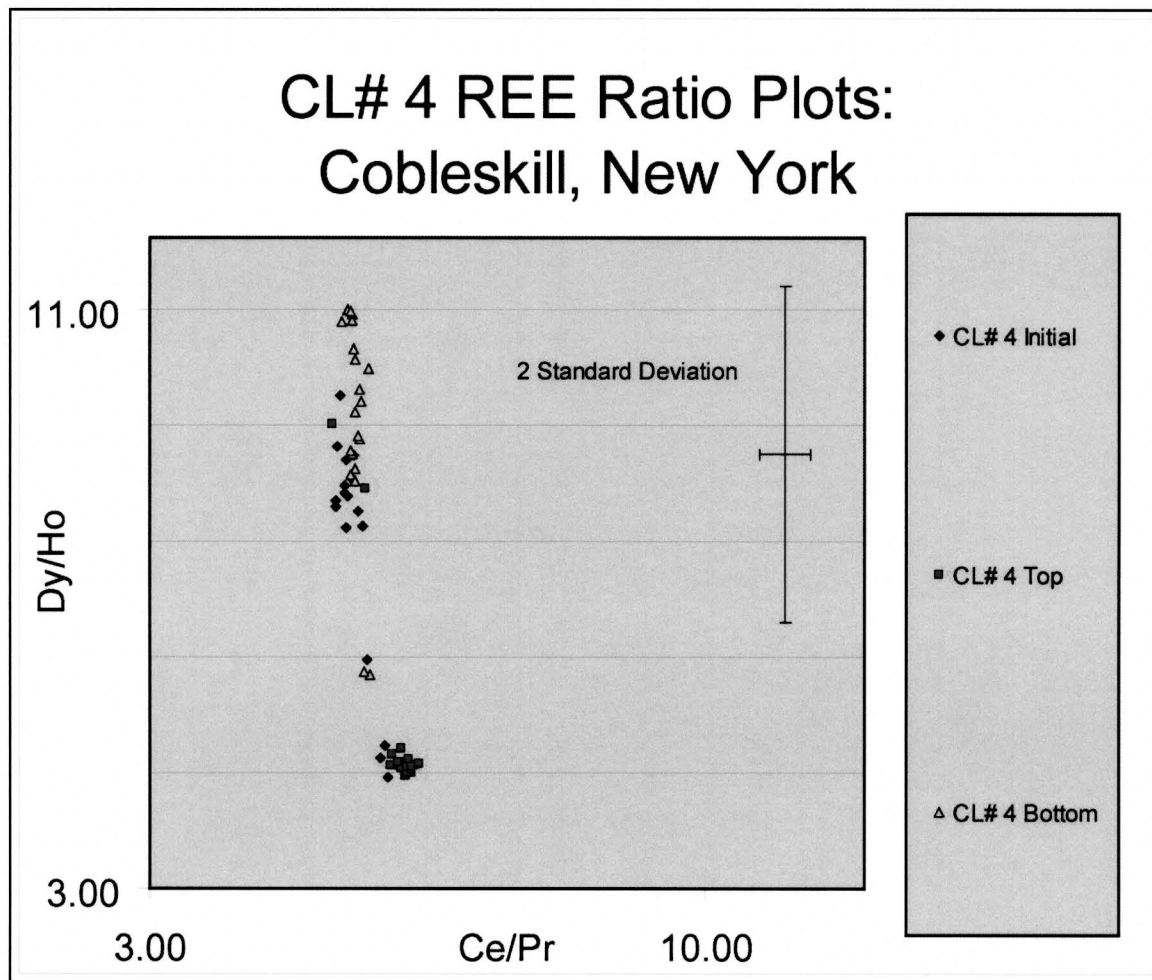


Figure 21: Rare earth element ratio plot for layer CL# 4 from values listed in APPENDICES B.4.3; B.4.6; and B.4.9. Data populations from CL# 4 have been subdivided and labeled based on initial samples taken in 2003 versus those resampled in 2004. Note that most data from the CL# 4 Bottom subdivision (yellow triangles) from the 2004 samples are significantly different than the CL# 4 Top subdivision (Red squares) from the same sampling date. Scale and legend are given.

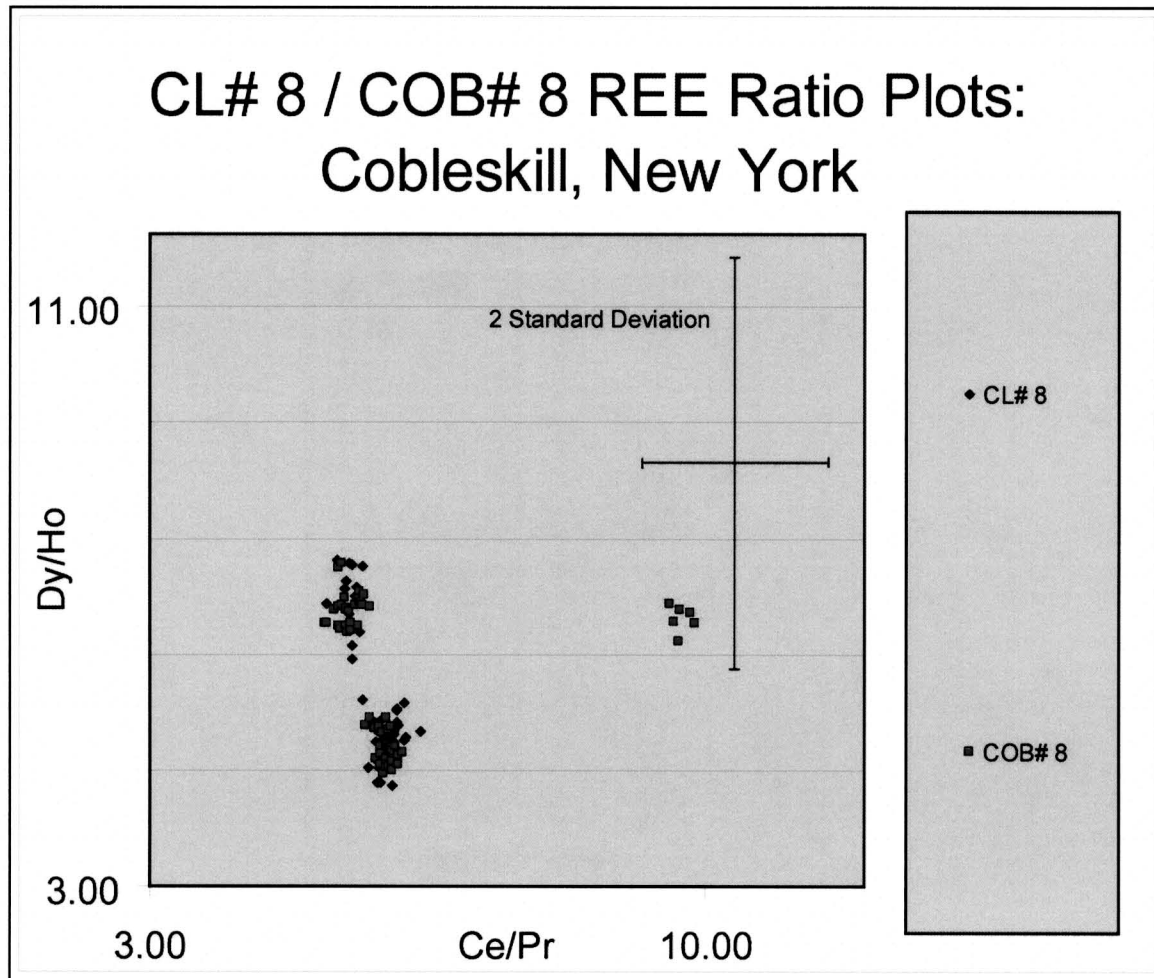


Figure 22: Rare earth element ratio plot from individual apatite phenocrysts obtained from the Esopus Sprout Brook K-bentonite layer CL# 8 at Locality A. Ratio plots from layer CL# 8 are from this study. Layer COB# 8 and corresponding plots are from the same volcanic layer. The crystals labeled COB# 8 were from the same outcrop location, but from a trench directly adjacent to the one in this study and analyzed separately by Dr. George H. Shaw.

These overlapping populations from the two separate samples and analyses corroborate the precision of the analytical method over time. They both show evidence of two different populations of apatite crystals in this single layer.

Figure 20 shows that layers CL# 4 and COB# 4, sampled from the same bed, also have multiple distinct, closely spaced crystal compositional populations based on the geochemistry of all individual apatite phenocrysts extracted from the layers.

Initially, samples of CL# 4 were taken in the summer of 2003. These samples were processed and geochemical data were eventually obtained (Figure 20 (CL#4), Figure 21 (CL# 4 Initial)). During the summer of 2004, the bed was resampled taking samples of both the top half and the bottom half of the layer. The resampling of this bed was an effort to obtain a sample unaffected by modern diagenetic processes, and therefore could be subdivided into multiple layers. Each subdivision was processed separately and the results are shown in Figure 21. This plot compares the initial (2003) samples to those resampled (2004) and shows that the upper and lower halves of the layer show different signatures and each population has a tight clustering with little scatter.

In addition, CL#8 from Locality A shows a similar pattern of varying crystal signatures when compared to layers CL#2 and CL#4. This layer showed more of a scatter among all the crystals analyzed, and distinct population clusters were singled out to show population separation. Additionally, data from this interval show another

slight population cluster on the right-hand part of the plot which has not been observed in beds CL# 2 or CL#4.

Apatite crystals obtained from the well documented and extensively studied Tioga B K-bentonite (Conkin and Conkin, 1979, 1984; Dennison, 1983, 1986; Smith and Way, 1983; Brett and Ver Straeten, 1994) from the Seneca Stone Quarry site (Locality D) also show trace element variations among volcanic phenocrysts (Waechter, 1993; Waechter et al., 1993; Shaw, 2003). Samples of the Tioga B were taken from the east wall of the quarry and are herein referred by the acronym SF, for Seneca Falls, then followed by the stratigraphic interval, in centimeters, of the sample. These numerical subdivisions are based on physical variations seen in the field. A schematic representation of these observations is displayed in Figure 23. Geochemical analyses indicate that the two subdivisions of the Tioga B K-bentonite bed, similar to the Sprout Brook K-bentonite beds, also exhibits more than one crystal population. Figures 24 and 25 show the ratio plots of these.

Once geochemical data from the Tioga B K-bentonite at Locality D was obtained, subdivisions (designated by letters a, b, c, and Clr.) were determined based solely on the geochemical signature of separate crystal populations. Each subdivision has separate crystal population signatures within them. For example, Figure 24 shows that SF 5-8 has two separate crystal populations. These populations were impossible to determine in the field, but when analyzed geochemically, the two subdivisions were given letters a and b. In addition, the subdivision SF 5-8 (Clr) was made due to a second

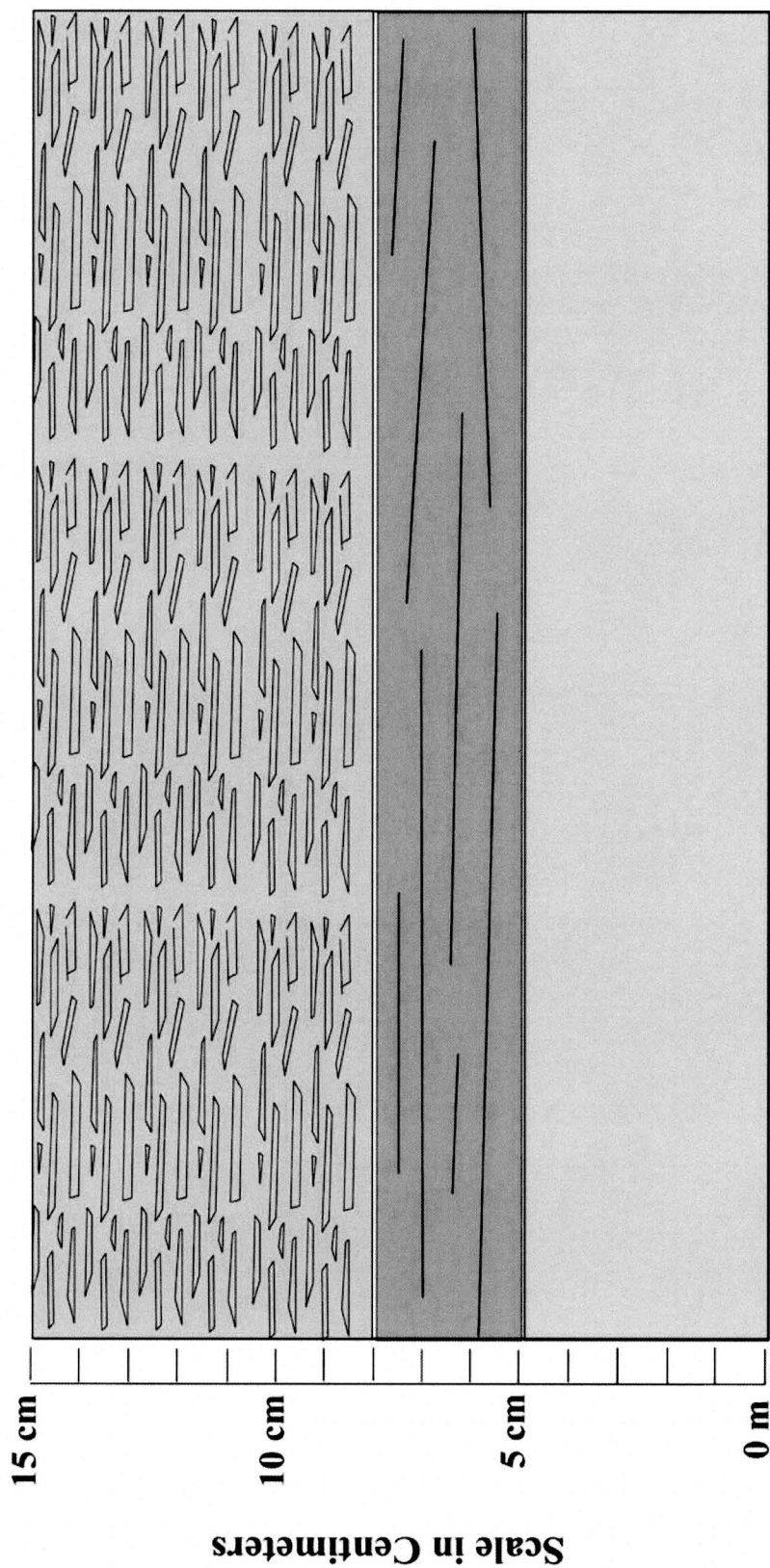


Figure 23: A schematic representation of the physical variations between the three subdivisions of the Tioga B K-bentonite at the Seneca Falls site (Locality D). The lower 5 cm is a clay rich interval. Lines within the 5-8 cm interval indicate a compact clay layer. The upper 7 cm subdivision contains large amounts of brittle clay fragments. Scale is provided.

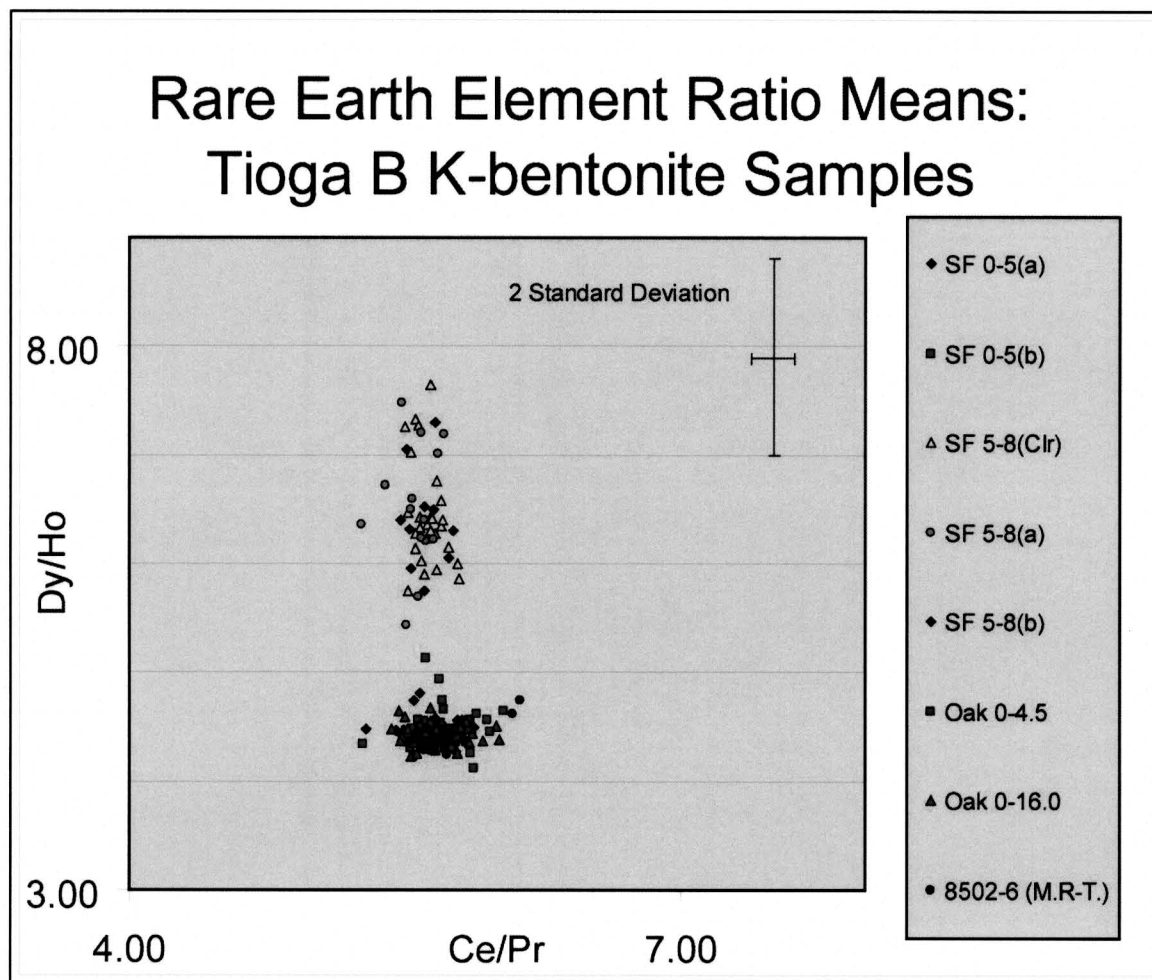


Figure 24: REE Ratio plots for all samples taken from Locality D for this study. The series "8502-6" are crystals collected by Dr. Mary Roden-Tice from the same bed, then analyzed by Dr. George H. Shaw (2003).

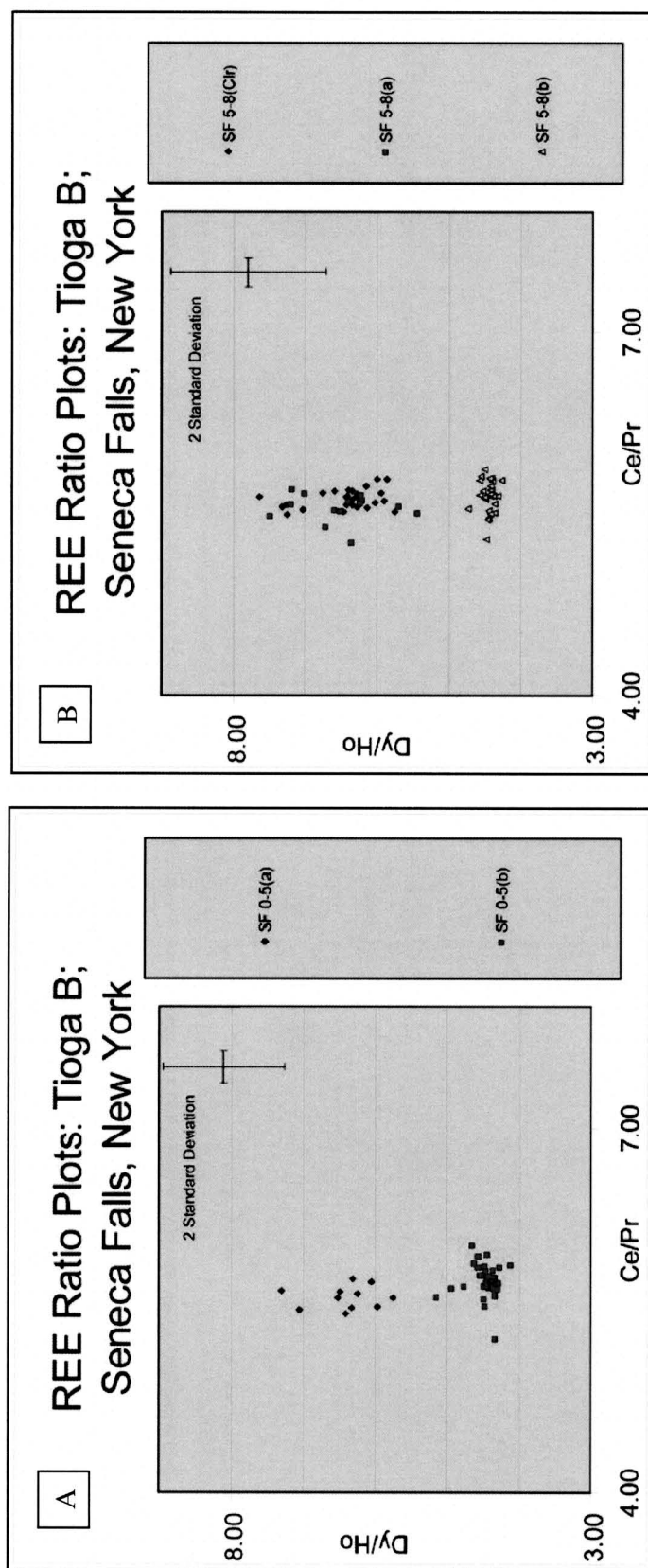


Figure 25: REE ratio plots for numerical subdivisions SF 0-5 (A) and SF 5-8 (B) of the Tioga B K-bentonite from the Seneca Stone Quarry (Locality D)

population of apatite phenocrysts that had a different color. One population was clear and colorless where the other was slightly clouded with a slight bluish tint. However, when attempting to analyze the second population of crystals from SF 0-5, no data were usable due either crystal misidentification during picking or the absence of apatite crystals in the polyethylene tubes during geochemical analysis.

Geochemical information was also obtained from apatite phenocrysts separated from the Tioga B K-bentonite from the Auburn (Locality C) southwest of Auburn, New York. Figure 26, unlike Figures 24 and 25, does not show any geochemical variation between separate crystal populations within the two divisions of the Tioga B K-bentonite bed at this locality. Both Oak 0.4.5 and Oak 0-16.0 show similar ratio signatures.

Lastly, apatite phenocrysts were analyzed from layers 7 Fount 1, samples a-c, and 7 Fount 3 from the Seven Fountains site (Locality G). Figure 27 shows a similar pattern as seen in Figure 26 where no apparent distinction between the elemental signatures within the individual K-bentonite layers collected from Locality G. These data also show there is no apparent separation among the geochemical signatures within apatite crystals from the two separate K-bentonite beds at Locality G, which are separated by more than 25 meters. Additional geochemical information on this locality and all others can be seen in Appendix B.

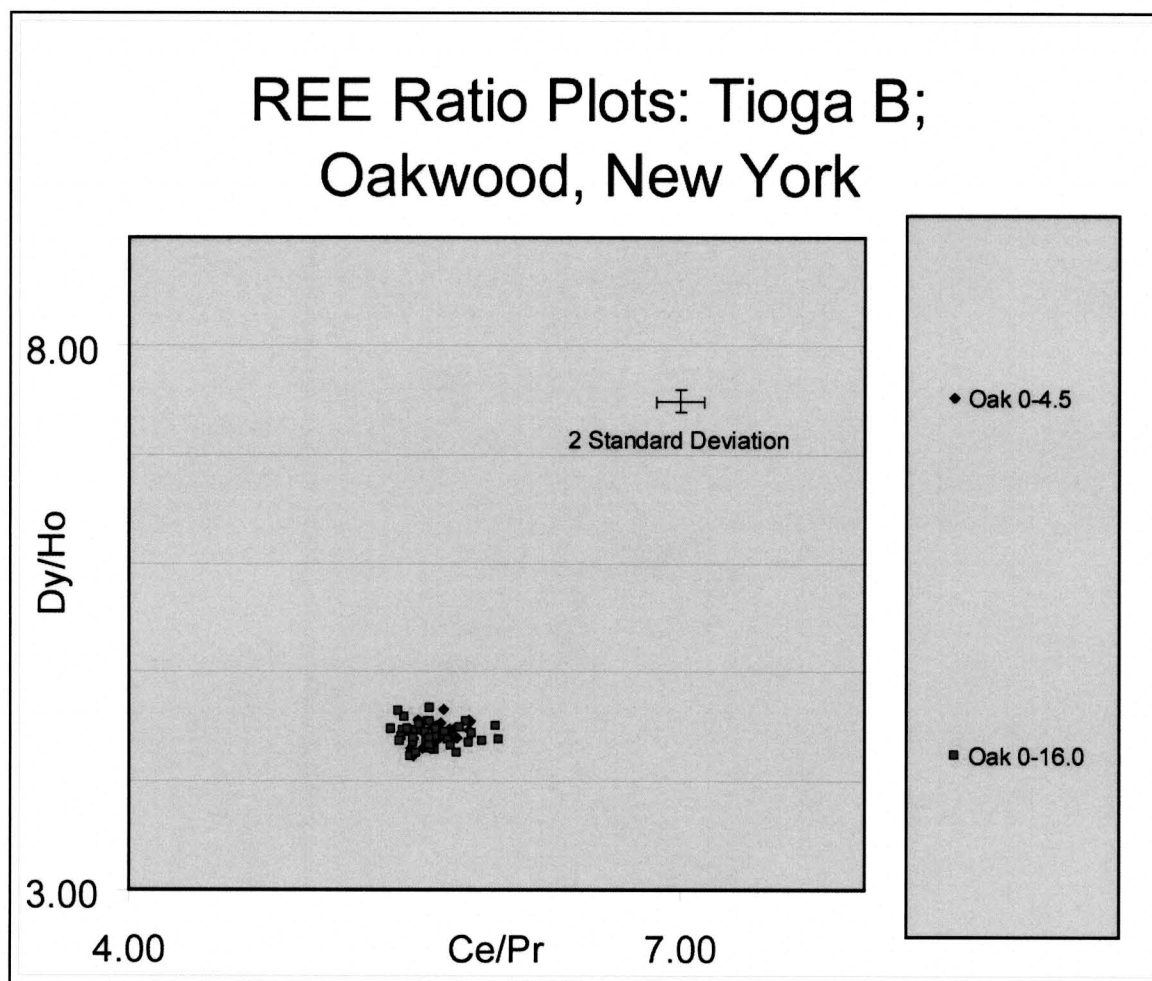


Figure 26: REE Ratio plots for both samples of the Tioga B K-bentonite taken from Locality C.

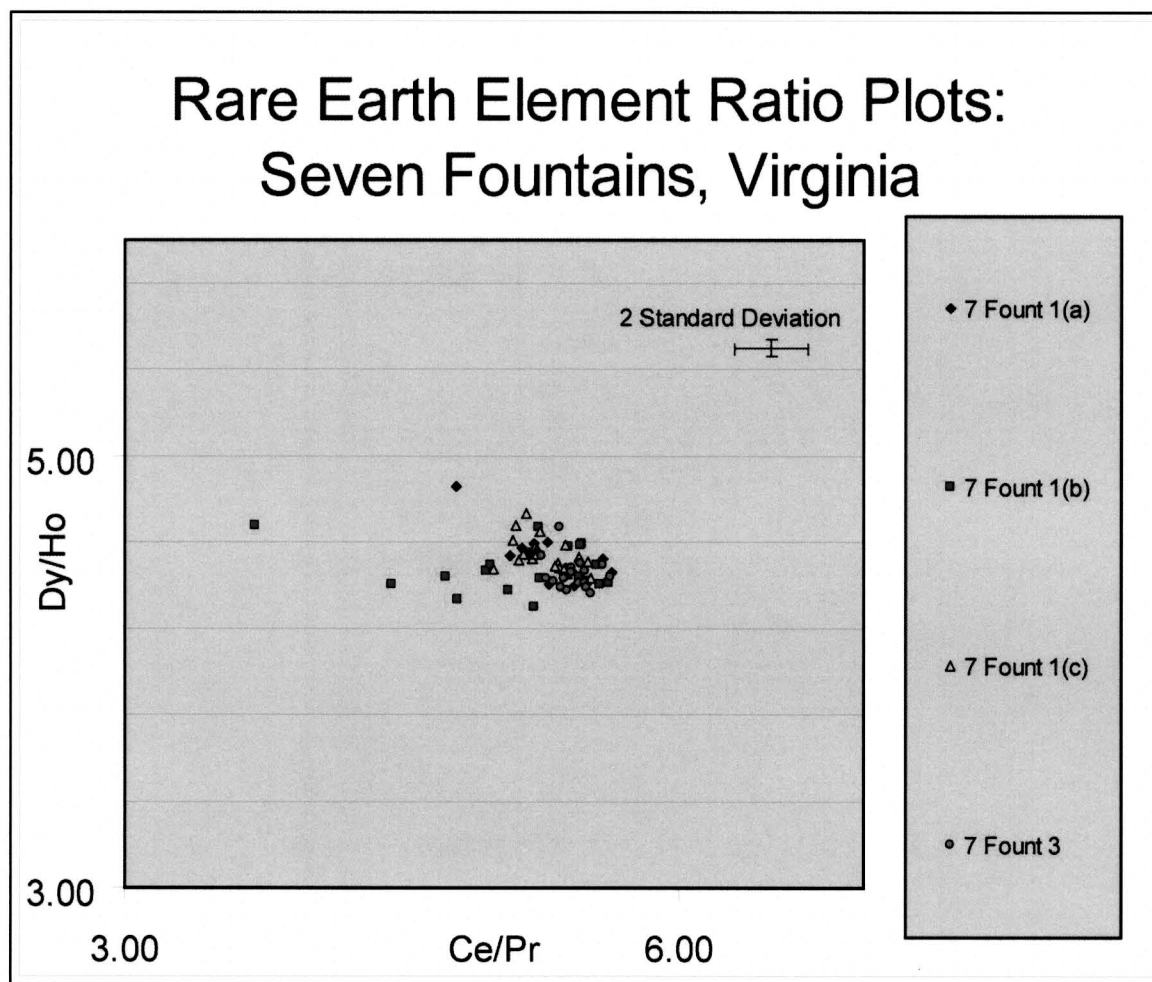


Figure 27: REE Ratio plots for all samples analyzed from Seven Fountains (Locality G).

STATISTICAL EVIDENCE

The geochemical evidence seen from trace and REE concentration data plots from the K-bentonites collected from Localities A, C, D, and G can also be completed by statistically comparing data from each locality and their various layers and/or subdivisions individually. The Tukey-Kramer HSD test is essentially a quantitative way to test the population separations that we see in the REE plots. The letter X in Tables 2, 3, and 4 shows that those beds in the upper left-hand corner of the data set can be geochemically distinguished from the bed at the top of the set of columns by using the apatite REE geochemistry. The more X marks that are present in a given data set, the more likelihood that the chemistry within crystals from the layer are significantly different than those of an adjacent subdivision of the same layer or another layer from the same sampling site.

DISCUSSION

K-bentonites of the Early and Middle Devonian portion of Earth's history represent significant planes yielding important information about the depositional history and preservational potential of these beds in varying depositional environments of the Devonian. They also give us clues to a variety of physical and biological processes and mechanisms occurring during the times when they were deposited. Many of the beds analyzed in this study show both physical and geochemical characteristics demonstrating that the layers represent more than just the altered remains of single eruptive events.

Table 2: The Tukey-Kramer HSD test for all layers sampled at Locality A. Note that an "X" indicates that a particular mean REE ratio values for all crystals from the layer in the upper left-hand corner of the individual data set box is significantly different from the layer along the top of the data set.

[illegible]

Table 3: The Tukey-Kramer HSD test for all layers sampled at Locality D. Note that an “X” indicates that a particular mean REE ratio values for all crystals from the layer in the upper left-hand corner of the individual data set box is significantly different from the layer along the top of the data set.

7 Fount 1(a)	7 Fount 1(a)	7 Fount 1(b)	7 Fount 1(a)	7 Fount 1(b)	7 Fount 1(c)	7 Fount 3
Ce/La		Ce/La				
Ce/Pr		Ce/Pr				X
Nd/Pr		Nd/Pr				
Nd/Sm		Nd/Sm				
Gd/Sm		Gd/Sm				
Gd/Tb		Gd/Tb				X
Dy/Tb		Dy/Tb				
Dy/Ho		Dy/Ho				X
Er/Ho	X	Er/Ho	X	X		X
Er/Tm		Er/Tm				
Yb/Tm		Yb/Tm			X	X
Yb/Lu	X	Yb/Lu				X
7 Fount 1(c)	7 Fount 1(a)	7 Fount 3	7 Fount 1(a)	7 Fount 1(b)	7 Fount 1(c)	7 Fount 3
Ce/La		Ce/La				
Ce/Pr		Ce/Pr		X		
Nd/Pr		Nd/Pr				
Nd/Sm		Nd/Sm				
Gd/Sm		Gd/Sm				
Gd/Tb		Gd/Tb	X			
Dy/Tb		Dy/Tb			X	
Dy/Ho		Dy/Ho			X	
Er/Ho	X	Er/Ho	X			
Er/Tm		Er/Tm				
Yb/Tm	X	Yb/Tm		X		
Yb/Lu	X	Yb/Lu	X	X	X	

Table 4: The Tukey-Kramer HSD test for all layers sampled at Locality G. Note that an "X" indicates that a particular mean REE ratio value for all crystals from the layer in the upper left-hand corner of the individual data set box is significantly different from the layer along the top of the data set.

VARIATIONS IN BEDDING

Field Observations

K-bentonite layers have been presumed to represent the remains of single eruptive events where the volcanic ashfall material is deposited and then ultimately preserved with little or no disruption or alteration. Presumably, stratification in a waterlain ash layer formed by settling would be horizontal. Recently, it has been shown that at least some of these layers appear to record depositional and eruptive histories far more complex than previously considered. During the deposition and preservation of a K-bentonite, a number of different stratigraphic factors can affect the layer (Ver Straeten, 2004).

The 7 Fount 2 layer from Seven Fountains site (Locality G) (Figure 12) is an example of how a volcanic layer can record a complex depositional history. In the photograph, arrows point to areas or lenses of finer grained material that alternates with the coarser, mica rich materials making up a majority of the layer. These fine-grained lenses could be interpreted in several ways.

First, these lenses of fine-grained material could separate layers representing primary laminae from a single event. The alternating fine and coarse-grained material in the layer suggests that the layer represents one recording both higher and lower energy conditions. These lenses may be evidence of sedimentary features resembling small-scale hummocky cross stratification indicating that storm activity may have influenced the layer at the time of final deposition. These wavy separations in the layer could be the result

of multiple, high energy storm events above the storm wave base that carried coarser material in, and as the events concluded, the quieter environmental conditions enabled deposition of the finer grained material.

These lenses of fine-grained material could also indicate the separation between multiple events and the layer represents the preservation of more than one primary depositional event. The event could be either more than one volcanic event, or pulses of the same volcanic event where the coarser grained material was deposited, followed by a period of quieter depositional conditions that promoted deposition of the fine-grained material afterwards.

The 7 Fount 2 K-bentonite bed is also heavily burrowed in portions of the layer. Multiple, small traces, indicative of burrowing, are present. This demonstrates that bioturbation of the soft sediment was a factor following deposition of the layer.

The 7 Fount 2 layer most likely did not record quiet settling conditions that typify normal waterlain ash layers, and by no means records a simple depositional history. It is possible that these features are due to the combined influences of wave and water flow regimes during storm events in the middle to outer shelf type depositional setting of the area during the Devonian (Ver Straeten, personal communication).

The three-layered volcanic layer 7 Fount 1, subdivisions (a)-(c), from Locality G (Figures 13, 14) is another bed showing a physical evidence of a complex depositional history. A volcanic layer deposited in a marine environment ought to have the heaviest

and most dense grains settle to the floor of the water body first. Then, deposition of the heaviest grains is followed by the smaller, less dense grains, and eventually the vesicular pumice (Fisher and Schminke, 1983; Königer and Stollhofen, 2001). Even if the larger micaceous grains were aerodynamically retarded and therefore took additional time to settle out of suspension, these crystals should have settled out prior to a majority of the finer grained volcanic ash material. If these grains were slow to settle out of suspension, then there would be evidence of larger micas throughout the layer. However this is not observed in the bed. This bed shows differing grain sizes in all three subdivisions of the layer that show no simple pattern. The uppermost subdivision of this layer, 7 Fount 1(c) has the coarsest grains, the next interval down, 7 Fount 1(b), has the finest grains of the three subdivisions and the lowermost, 7 Fount 1(a) has intermediate size grains. This upward fining then back to coarsening suggests the possibility that this layer is depositionally complex. The bed may have been influenced by physical processes during or after deposition, or is the result of more than one eruptive event.

Fossils

The presence of a fossil layer within a K-bentonite bed implies that the K-bentonite bed may contain material from two or more separate depositional events. There would have to be a nondepositional period between these events long enough to sustain faunal colonization. The presence of chonetid *Hallinetes halli* brachiopod fossils within the Tioga B K-bentonite from both

Localities E and F support the idea of a colonization event during the deposition of the Tioga B K-bentonite. These fossils might have been preserved *in situ* and been buried under the volcanic ash material deposited in the marine environment during the second event. In both localities, the presence of these fossils could represent the division of two separate eruptive events; one event contained no fossils and another event incorporated fossils from a colonization event that were buried.

Another possibility is that the marine fossils observed within the Tioga B K-bentonite may have been transported into the depositional environment from somewhere in close proximity due to a storm-generated event. A storm event would increase the water energy and disturb the layer, not only reworking the layer itself, but also transporting fossils from another location into the redeposited K-bentonite. If a storm event washed the fossils into the area, then the fossils would most likely show no preferred orientation. In addition, fossils within the Tioga B K-bentonite could be the result of the reworking of soft sediments below the Tioga B K-bentonite bed. If the upper portion of the Moorehouse Member of the Onondaga Formation contained these chonetid brachiopod fossils, and was still soft sediment, then it is possible the fossils came from the layers below the Tioga B. This softer upper Moorehouse, along with a newly deposited Tioga B K-bentonite, could have been reworked during a storm event, redistributing the material into what is currently seen in the field.

However, we observe the presence of fossils in the Tioga B K-bentonite in more than one locality, and we see it over significant distances. The apparent life position of the chonetid *Hallinetes halli* brachiopod fossils within a Tioga B K-bentonite from the Echo Lake and Stroudsburg sites (Localities E and F) indicates that the Tioga B does not represent a reworked K-bentonite bed. Other localities described in Ver Straeten (2004) from New York, also show the presence of brachiopods, and in some cases bryozoan fossils, within this K-bentonite. In addition, due to the delicate nature of some of the bryozoan fossils found at the Honeoye Falls location (Ver Straeten, 2004) it is also unlikely that a storm generated event carried these from another area since most of the observed fossils seem to be intact; a storm event could destroy these fossils. Considering the geographic extent of these fossil observations and the delicate nature of some of the fossils, it is interpreted that the Tioga B shows a complex depositional history (Ver Straeten, 2004; Ver Straeten, personal communications). Of course the upper portions of the Tioga B ash could be reworked along with terrigenous sediments, however, there should be an appearance of more mixed carbonate sediments along with the terrigenous material. If the Tioga B K-bentonite and layers below it were reworked by a storm event, it is likely that these background carbonate sediments would be seen. However, carbonate material of this nature has not been observed.

Thin Sections

Samples of the "chrome bed" from Locality H show variations in

the abundance and orientation of muscovite crystals in the tuffaceous sandstone. The lower portion of the bed there contains coarse muscovite and other volcanic crystals including quartz and feldspar (Figure 17(a)). This portion of the slide contains less abundant muscovite, where few of these grains are flat lying, possibly indicating a difference in the conditions in the depositional environment. Turbulent water conditions during deposition may have influenced the muscovite grain orientations while settling out of the water column. Alternatively, this lower section could have been influenced by increased amounts of biological disruption and reworking after deposition, or the lower portion of the chrome bed may have been reworked by a storm-generated event.

Second, in the upper portion of the bed (Figure 17(c)), there is a band of tightly spaced, flat-lying, dark brown muscovite grains. The orientation of these grains may indicate calmer depositional conditions with decreased turbulence during accumulation the ashfall material. Less turbulent water conditions would increase the likelihood that grains would settle out of suspension without any difficulty. The horizontal orientation of the muscovite grains in the upper portion of the bed would also indicate little to no burrowing of the layer after deposition.

A finer grained layer of iron hydroxide minerals (Figure 17(b)) appears to separate the upper muscovite seam from the lower portion of the thin section. This fine-grained boundary could indicate a decrease in the water turbulence during deposition. This

decrease would allow finer grained particles to settle out of suspension. This horizon could also indicate a boundary between two separate eruptive events. The finer grained material may alternatively represent background sediments deposited between eruptive events as the volcanic ash material became less available.

Thin sections from the Tioga B at Locality F show physical variations indicating a complex depositional history. Slides of the bottom 25 cm show tightly stacked, flat lying biotite crystals. This orientation could indicate a sedimentary environment with calmer water condition where the grains had time to settle out of suspension slowly. These biotite grains are more abundant, and no trace fossils or other fauna can be seen. The absence of fossils could indicate deposition of increased amounts of volcanic material resulting in a layer that burrowing organisms could not penetrate.

At the boundary between the upper and lower sections of the sample from Locality F, there is a color change in the rock, and an increase of trace and shelly marine fossils is apparent. The finer grained matrix in the upper portion of the layer is much darker than the lower portion of the bed. This color change could indicate different cements where the upper 25 cm is dominated by more calcareous cement where the lower 25 cm contains more siliceous cement. Also, the abundance of biotite grains within the upper 25cm of the bed declines dramatically, and those biotite grains present do not have the same consistent horizontal orientation as those found in the bottom 25 cm. Abundant post-depositional burrow traces and shelly marine fossils are found scattered throughout the upper

25 cm of the Tioga B K-bentonite bed indicating a change in seafloor conditions that probably supported colonization of the layer by marine organisms, or perhaps burrowing organisms reworked the deposit down as deep as 25 cm after the deposition of the volcanic material. These features demonstrate that the environmental conditions changed during the deposition of the Tioga B K-bentonite at Locality F.

GEOCHEMISTRY OF APATITE PHENOCRYSTS

Studies have shown that analyzing the geochemistry of volcanic phenocrysts can be extremely useful when examining the volcanic characteristics of the phenocryst and the layer that contains these crystals (Samson et al., 1988, 1990; Delano et al., 1990; Schirnack, 1990; Lindstrom et al., 1992; Waechter, 1993; Waechter et al. 1993; Delano et al., 1994; Hansen, 1995; Dannenmann 1997; Shaw, 2003). Among other resistant crystals, apatite phenocrysts are present in most K-bentonites and contain trace amounts of rare earth elements (REE) that vary from magma to magma in absolute abundance and in light to heavy REE ratios. Similar to the quartz phenocrysts used for melt inclusion geochemistry (Delano et al., 1990; Schirnack, 1990; Lindstrom et al., 1992; Waechter, 1993; Waechter et al. 1993; Delano et al., 1994; Hansen, 1995; Dannenmann 1997), apatite has a high survival potential and the composition is likely not to change significantly during the alteration of ash. Classically, K-bentonites have been considered the altered remains of single eruptive events. Presumably, if this idea holds true, then the geochemistry of phenocrysts contained within a single layer would

have the same chemical signature. Therefore, if this presumption is right, all crystals contained within a supposed single layer should be geochemically identical. If varying or multiple compositional populations are found within a layer, this could demonstrate that the layer does not in fact represent a single ash, but is a combination of one or more ashfall events that may have additionally been reworked by a number of physical and biological (stratinomic) factors (Ver Straeten, 2004).

Crystals that are from the same host magma will have similar geochemical characteristics. Therefore, even when the crystal weight of those phenocrysts being analyzed cannot be determined for weight percent and absolute concentrations of the analytes used in the study, crystals of the same chemistry will exhibit the same proportion of these key trace elements within themselves. Even if the crystals were formed in conditions indicating magma chamber variations, i.e. zoned magma chamber, the layer should have only one crystal population fingerprint (G. Shaw; M. Lupulescu; J. MacDonald, personal communication). However, when we examine the data from many of the localities in this study, we see data that do not conform to this model.

In this study the geochemistry of individual apatite crystals was analyzed to test interlayer and intralayer homogeneity. Once trace element data is obtained for a layer using ICP-MS, adjacent REE element concentration values are used to construct ratios in order to show possible interlayer and intralayer variability. Adjacent REE elements were analyzed sequentially to reduce error due

to instrumental drift. In addition, heavy REE concentrations are low in apatite crystals and the use of ratios that compare light versus heavy REE are less accurate. ICP-MS provides statistical information on populations of grains and these methods can show both interlayer and intralayer chemical variability (Shaw, 2003).

The separation of the two or more discrete fingerprints of crystal populations within layers CL# 2, CL# 4, and CL# 8 at Locality A indicates that these layers are not simply the remains of a single eruptive event, but that they most likely represent the mixing of separate ashfall events. The evidence from these three plots (Figure 19, 20, 22), in addition to more plots found in Appendix B using other trace element ratios, demonstrate that many of the beds studied at Locality A do not represent single events, but multiple events that may have been separated by low sedimentation rates during the time between eruptions (Königer and Stollhofen, 2001). Additional data from the ICP-MS analyses of the Sprout Brook K-bentonite layers from Locality A can be found in Appendix B.

The K-bentonite beds from the Sprout Brook K-bentonite cluster have yielded the most geochemical information of all samples analyzed in this study. Of all the beds in the cluster, three beds were analyzed, but most interesting is the geochemical signature from K-bentonite layer CL# 4 of the Sprout Brook K-bentonites from Locality A. It was determined that the geochemical signature of the bed was distinctly different at the bottom of the bed when compared to the top. This kind of evidence strongly supports the idea that

this layer contains volcanic material from two separate eruptive events, most likely followed by a post eruptive depositional hiatus in the time between eruptions, complemented by a low rate of sedimentation and little ash reworking during that interval.

Anomalous geochemistry

7 Fountains, Virginia

Rocks of the Needmore Formation (Selinsgrove Member) found at the Seven Fountains site (Locality G) are interpreted to be time equivalent to the limestones of the Onondaga Formation in New York (Ver Straeten, personal communication). The geochemistry of two layers were analyzed from this site. The first (7 Fount 1) is a 15 cm K-bentonite layer that was subdivided into three-5 cm layers (subdivisions a-c) based on varying physical features. These samples are from the interpreted equivalent to the upper part of the Edgecliff Member of the Onondaga Formation. This layer has been discussed previously based on varying physical characteristics that indicate the layer possesses evidence of a complex history. Each subdivision was processed and analyzed separately using the ICP-MS analytical method.

A second layer studied (7 Fount 3) is significantly higher in the section located more than twenty meters above the first sample. In the field, this bed is a brittle 8 cm-thick tan to khaki compact clay with visible mica crystals. This bed occurs within strata correlative to the lower part of the Moorehouse Member of the Onondaga Formation (Ver Straeten, personal communication).

When analyzed, the two layers (7 Fount 1 and 7 Fount 3) from Seven Fountains (Locality G) should have different chemical compositions based on their stratigraphic separation. However, the geochemical ratios and the light versus heavy REE plots (see Figure 27), we see that these layers show a strikingly similar chemistry with crystal ratios overlapping each other. Up to this point, there is no explanation for this anomaly.

Tioga B: Seneca Stone Quarry

Geochemical data obtained from layer samples of the Tioga B at the Auburn site (Locality C) supports findings in Shaw (2003) showing little or no variation in the geochemical fingerprint from apatite phenocrysts from multiple localities of the Tioga B throughout Pennsylvania and New York. However, the varying trace and REE data obtained from the Tioga B K-bentonite from the Seneca Stone Quarry site (Locality D) is anomalous. While the geochemical data in this study is not supported by the findings of Shaw (2003), it may be supported by other studies concerning the geochemical fingerprint of the Tioga B K-bentonite. Trace element data from rhyolitic melt inclusions contained within the Tioga B K-bentonite shows a bimodal distribution in the geochemical signatures of crystals within the K-bentonite bed (Waechter, 1993; Waechter et al. 1993). This data supports the idea that the Tioga B records a complex eruptive history, however, further sampling and analysis of the bed is needed to check for any possible procedural or analytical errors in sampling.

Possible geochemical biases

There is the possibility that even though a difference is seen within a certain layer, interlayer variability could be caused not by multiple eruptive events, but by other factors. First, magma chamber differentiation could be the cause of the population separation seen in the trace element chemistry plots. Hervig and Dunbar (1992) looked at fluid inclusions in pumice lumps to see if magma mixing occurred in the Bishop and Bandelier Tuffs in the Southwest, United States. In order to exclude magma chamber differentiation and variation, one could use heavy REE versus light REE to distinguish magmatic characteristics between crystals (Rollinson, H. R., 1993; Sun, S. S., McDonough, W. F., 1989; McDonough, W. F., and Sun, S. S., 1995; James MacDonald, personal communication). Results from this test can be seen in Figure 28 which compares ratios of cerium/praseodymium versus lanthanum/lutetium for the Sprout Brook bentonite cluster layers from Locality A.

Populations of crystals with similarities in magma chemistry will have similar slopes on this diagram. However, if the data have different slopes, it supports the idea that these are from two (or more) eruptive sources. In Figure 28 the geochemical signatures from the apatite crystals do not show the simple pattern indicating a single magma chemistry is present. The presence of more than one population in this figure suggests the idea that more than one magma signature is present. This comparison in the layers from Locality A is evidence that the layers from this locality show a complex

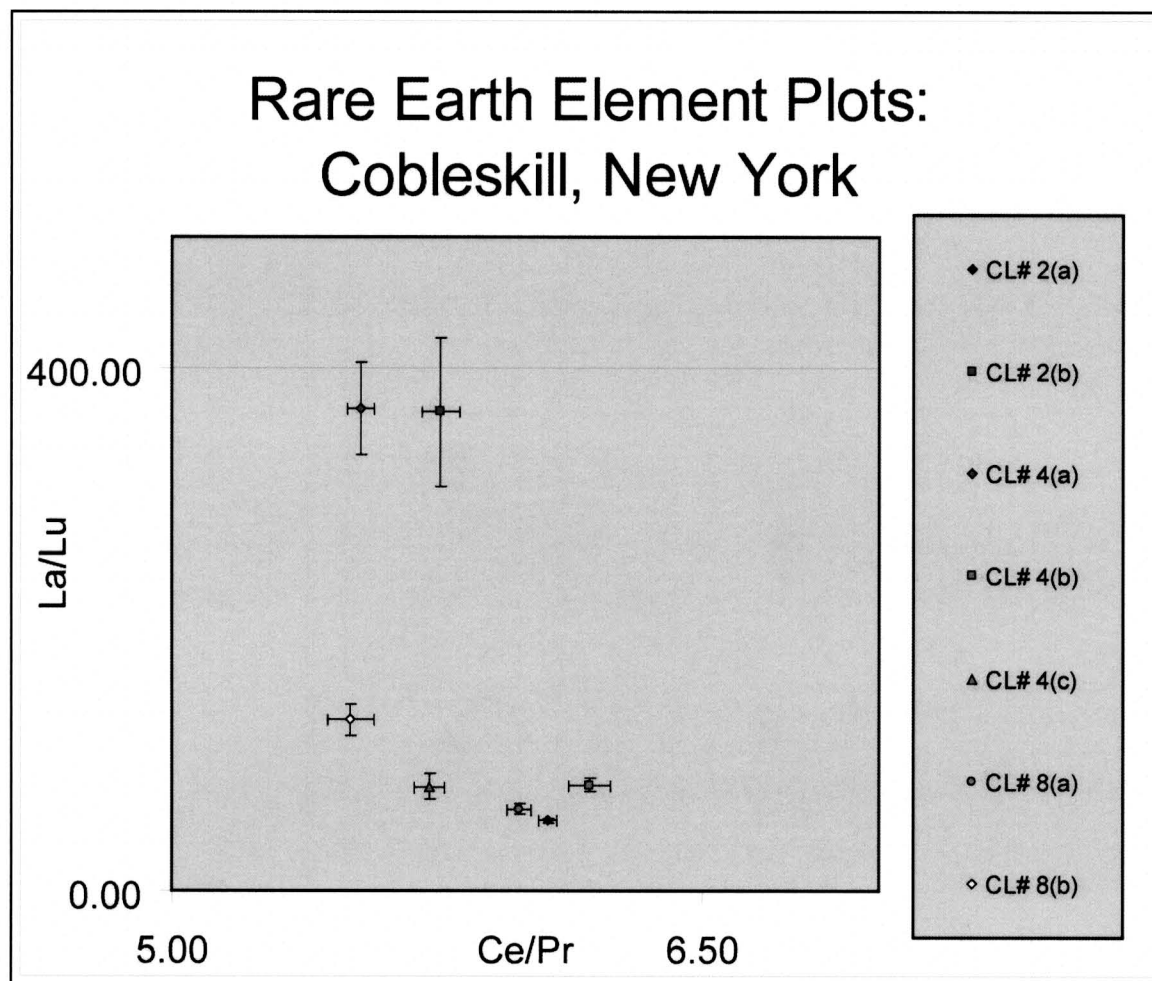


Figure 28: Mean plots of Heavy REE versus Light REE for layers CL# 2, CL# 4, and CL# 8 sampled at Locality A in order to distinguish magma characteristics within layers from the same locality. Separate populations indicate the La/Lu enrichment in a given layer, therefore implicating varying magma geochemistry within a single layer. 2 Sigma error bars are shown.

eruptive history based not just on this test, but also because of the separation of the fingerprints of apatite crystal populations seen in Figures 19 through 22.

This geochemical method presumes that the apatite crystals analyzed are in fact all of volcanic origin. The K-bentonite layers in this study were deposited in marine depositional environments varying in sediment type and availability, water depth and turbulence, and biological activity. The underlying sediments most likely contain amounts of volcanic material from prior eruptive events that have been eroded and transported to the area and/or been biologically dispersed by burrowing organisms. This scenario could have resulted in the incorporation of detrital apatite crystals into the layer as it is being deposited.

A new study by Shaw (personal communication) uses REE and trace element analyses to test whether the apatite separates are detrital in origin or of primary volcanic character. In his study, he analyzed apatite phenocrysts from both bentonite layers and from sandstone beds from the Great Valley Sequence of California to see how these crystals plot when using the analytical method used in this study and in Shaw (2003). Shaw found that apatite crystals from sandstones contained multiple chemical signatures that do not compliment each other and have increased amounts of scatter. Conversely, when apatite crystals from a bentonite were analyzed, the ratios plotted in a tight cluster with very little scatter. In this study we see compositional patterns that reflect primary

volcanic characteristic of bentonites, rather than crystals of detrital origin.

CONCLUSIONS

Sprout Brook K-bentonite Cluster

The physical and geochemical data and observations from the Sprout Brook K-bentonite Cluster at Locality A, show little to no physical data or observations that indicate a complex depositional history is recorded in the layers. However, there is a significant geochemical evidence for complex depositional history.

Trace and REE concentrations indicate that at least three of K-bentonite layers at Cobleskill (Locality A) show complex eruptive histories. Layers CL# 2, CL# 4, and CL# 8, all show more than one geochemical fingerprint within the individual layers. This pattern of two or more apatite population fingerprints strongly suggests that the single layers are in fact the combination of more than one eruptive event.

In addition, data in Figure 21 shows different crystal fingerprints within the layer CL# 4 when it is subdivided in half. This demonstrates, in the case of CL# 4, that this layer has incorporated crystals from more than one eruption and the two are superimposed on top of one another, with no distinguishable difference between the two visible (without the geochemical analyses).

The Tioga B K-bentonite

Geochemical data from the Auburn Quarry site (Locality C) and from Shaw (2003) indicate the geochemical signatures from multiple

samples of the Tioga B K-bentonite in both New York and Pennsylvania show consistent elemental concentrations within apatite phenocrysts supporting the idea of a simple eruptive history. Though geochemistry does not indicate multiple eruptive events, physical and paleontologic characteristics do. Observations from Localities E, and F, along with data listed in Ver Straeten (2004), show evidence that the Tioga B may not record a complex eruptive history but a complex depositional history. A multi layered Tioga B K-bentonite is seen as two to three separate K-bentonite layers at Localities E and F in eastern Pennsylvania, in addition to sites in western New York and possibly in western Virginia (Ver Straeten, 2004). Ver Straeten (2004) shows the Tioga B K-bentonite contains complex depositional features where the bed is represented as a multi layered K-bentonite bed, (Ver Straeten, 2004; his figure 3a) and contain marine fossil horizons within parts of the layer, (Ver Straeten, 2004; his figure 3c), both indicating a complex depositional history. In addition, Ver Straeten (2004) wondered if the Tioga B is represented at Seven Fountains, VA by three different layers, separated by shales. This would further support interpretations that the Tioga B represents multiple events, in contrast to geochemical data from Shaw (2003). However, without further analysis this interpretation is inconclusive.

Moreover, geochemical analyses from Waechter (1993) and Waechter et al.(1993) may further support the idea that the Tioga B K-bentonite represents a complex bed. In these studies, a bimodal distribution in trace elemental concentrations was found within

rhyolitic melt inclusions from the Tioga B K-bentonite. This data suggests that the eruptive material originated from a zoned magma, however, further analyses of the Tioga B K-bentonite are needed.

Seven Fountains, Virginia

The Seven Fountains site (Locality G) shows visible, physical evidence demonstrating that some of the layers are depositionally complex. We see that the 7 Fount 1 and 7 Fount 2 beds both show variations that support a complex depositional environment possibly affected by changing water turbulence in the area and varying biological activity. However, geochemical results from this site do not indicate a complex volcanic history.

SUMMARY

The physical and geochemical data obtained from this study demonstrates that many K-bentonite layers, no matter what their geologic age, can record a complex eruptive or depositional history. When examining a K-bentonite bed, one can interpret whether the layer records a simple history or one more complex. Many factors can affect the layer before its discovery and exhumation.

Based on physical observations, a complex K-bentonite bed could be the remains of a single eruptive event, but physically altered by varying environmental and biological factors that may make it difficult to identify. In the case of the Tioga B, physical variations in samples from multiple localities show that the K-bentonite records a complex depositional history affected by primary depositional factors as well as post-depositional stratigraphic processes in the area of deposition. In contrast to physical

evidence, geochemical analyses of this layer, from this study and from Shaw (2003), appear to indicate that the Tioga B does not record a complex eruptive history. Also, the Seven Fountains site shows physical evidence within multiple layers supporting a complex depositional history. But when geochemically analyzed, the signatures do not represent more than one eruptive event.

Conversely, analyzed beds from the Sprout Brook K-bentonite cluster at Locality A shows little physical evidence demonstrating a complex depositional history. This locality and the layers within it show geochemical signatures implicating more than one eruptive event. These K-bentonite beds represent the altered volcanic material from multiple eruptive events where more than one event are found in single K-bentonite beds.

This study and others regarding Devonian volcanic ash beds demonstrate the effectiveness of both physical observations, on macro and micro scale, and geochemical approaches to examine many volcanic layers. When examining information and observations from K-bentonite beds at a single layer or locality, noticeable physical and geochemical variations within layers in this study are supported by additional interpretations that some K-bentonites record a more complex eruptive history than previously thought (Huff et al., 1999; Ver Straeten, 2002, 2004). Additional analyses on the samples already obtained from Devonian sediments in the Appalachian basin are planned in order to strengthen the idea that these layers are more complex than previously determined. The apparent complex history that is recorded in the physical and geochemical results

from analyses on the beds in this study show that present interpretations regarding K-bentonites are incomplete due to the lack of acknowledgment of all stratigraphic factors that influence the beds during their preservation.

Modern studies have analyzed apatite phenocrysts and show that the crystals record an abundant amount of geochemical information that can be used to study the eruptive characteristics of many modern eruptions (Imai A., 1993; Peng, et al., 1997; ; Streck M.J., 1998; Baker L.L., 1996; Parat F., 2002). These studies further support the idea that apatite can be a useful geochemical tool and can show geochemical variations among separate crystal populations.

REFERENCES AND WORKS CITED

- Baker L.L., and Rutherford M.J., 1996, Crystallisation of anhydrite-bearing magmas: Transactions - Royal Society of Edinburgh: Earth Sciences, vol 87, no.1-2, p. 243-250.
- Brett, C.E., and Ver Straeten, C.A., 1994, Stratigraphy and facies relationships of the Eifelian Onondaga Limestone (Middle Devonian) in western and west central New York State: in Brett, C.E., and Scatterday J., eds., New York State Geological Association, 66th Annual Meeting Guidebook, p. 221-269.
- Conkin, J.E., and Conkin, B.M., 1979, Devonian pyroclastics in eastern North America, their stratigraphic relationships and correlation,: in Conkin, J.E., and Conkin, B.E., Devonian-Mississippian boundary in southern Indiana and northwestern Kentucky: Louisville, Kentucky, University of Louisville, Ninth International Congress of Carboniferous Stratigraphy and Geology, Field Trip 7, p. 74-141.
- Conkin, J.E., and Conkin, B.M., 1984, Paleozoic metabentonites of North America: Part 1-Devonian metabentonites in the eastern United States and southern Ontario: Their identities, stratigraphic positions, and correlation: University of Louisville Studies in Paleontology and Stratigraphy, no. 16, 136 p.
- Dannenmann, S., 1997, Analysis of glasses present in quartz and apatite phenocrysts from Ordovician K-bentonites in the Mohawk Valley, NY: [MS Thesis] Albany, State University of New York, 92 p.

- Delano, J.W., Schirnack, C., Bock, B., Kidd, W.S.F., Heizler, M.T., Putman, G.W., DeLong, S.E., and Ohr, M., 1990, Petrology and geochemistry of Ordovician K-bentonites in New York State: Constraints on the nature of a volcanic arc: *Journal of Geology*, vol. 98, p. 157-170.
- Delano, J.W., Tice, S.J., Mitchell, C.E, and Goldman, D., 1994, Rhyolitic glass in Ordovician K-bentonites: A new stratigraphic tool: *Geology*, vol. 22, p. 115-118.
- Dennison, J.M., 1983, Internal stratigraphy of Devonian Tioga ash beds in Appalachian Valley and Ridge province: *Geological Society of America Abstracts with Programs*, no. 15, p. 557
- Dennison, J.M., 1986, Tioga bentonite in the Appalachian Basin: Final report: U.S. Department of Energy, Contract No. EY-76-05-5195, 101 p.
- Dennison, J.M., and Textoris, C.A., 1970, Devonian Tioga tuff in northeastern United States: *Bulletin Volcanologique*, 34, 289-294.
- Dennison, J.M., and Textoris, C.A., 1978, Tioga bentonite time-marker associated with Devonian shales in Appalachian Basin,: in Schott, B.L., Overbey, W.K., Jr., Hunt, A.E., and Komar, C.A., eds., *Proceedings of the First Eastern Gas Shales Symposium*: U.S. Department of Energy, Publication MERC/SP-77-5, p. 166-182.
- Dennison, J.M., and Textoris, D.A., 1987, Paleowind and depositional tectonics interpreted from Tioga ash bed: *Appalachian Basin Industrial Associates Program*, 12, 107-132.
- Ebert, J.R., Applebaum, R.H.S., and Finlayson, H.C., 1992, K-bentonites and detrital mudstones in the Helderberg Group (L.Dev.), New York:

- Implications for tectonic versus eustatic cyclicity: Geological Society of America Abstracts with Programs, vol. 24, no. 3, p. 18
- Ettensohn, F.R., 1985, The Catskill delta complex and the Acadian orogeny: A model, in Woodrow, D.L., and Sevon, W.D., eds., The Catskill delta: Geological Society of America Special Paper 201, p. 39-49.
- Fisher, R.V. and Schminke, H.-U., 1984, Pyroclastic Rocks: Springer-Verlag, New York, 472 p.
- Hansen, B., 1995, A geochemical study of rhyolitic melt inclusions in igneous phenocrysts from Lower Devonian bentonites: [PhD Thesis] Albany, State University of New York, 470 p.
- Hervig, R.L., and Dunbar, N.W., 1992, Cause of chemical zoning in the Bishop (California) and Bandelier (New Mexico) magma chambers: Earth and Planetary Science Letter, vol. 111, p. 97-108.
- Hosterman, J.W., and Whitlow, S.I., 1983, Clay mineralogy of Devonian shales in the Appalachian Basin: U.S. Geological Survey Professional Paper P-1298, 31 p.
- Huff, W.D., Muftuoglu, E., Kolata, D.R., and Bergstrom, S.M., 1999, K-bentonite bed preservation and its event stratigraphic significance: Acta Universitatis Carolinae, Geologica, vol. 43, p. 491-493.
- Imai A.; Listanco E.L.; Fujii T., 1993, Petrologic and sulfur isotopic significance of highly oxidized and sulfur-rich magma of Mt. Pinatubo, Philippines: Geology, vol. 21, p. 699-702
- Königer, S. and Stollhofen, H, (2001), Environmental and tectonic

- controls on preservation potential of distal fallout ashes in fluvio-lacustrine settings: the Carboniferous-Permian Saar-Nahe Basin, south-west Germany: *in* White, J.D.L., and Riggs, N.R., eds., *Volcaniclastic Sedimentation in Lacustrine Settings*, Oxford, Special Paper no. 30, p. 263-284
- Lindstrom, D. J., Delano, J.W., Hanson, B.Z., and Waechter, J.W., 1992, Geochemical stratigraphy of Devonian sediments in New York and Pennsylvania using glass-bearing quartz phenocrysts: *Geological Society of America, Abstracts with Programs*, vol. 24, no. 7, p. 231
- McDonough, W. F., and Sun, S. S., 1995, The composition of the Earth: *in* McDonough, W. F., Arndt, N. T., and Shirey, S., eds., *Chemical evolution of the mantle, Chemical Geology*, vol. 120, p. 223-253.
- Osberg, P.H., Tull, J.F., Robinson, P., Hon, R., and Butler, J.R., 1989, The Acadian orogen, : *in* Hatcher, R.D., Thomas, W.A., and Viele, G.W., eds., *The Appalachian-Ouachita orogen in the United States*:. Boulder, Colorado, Geological Society of America, *Geology of North America*, F2, p. 179-232
- Parat F., Dungan M.A., and Streck M.J., 2002, Anhydrite, pyrrhotite, and sulfur-rich apatite: Tracing the sulfur evolution of an Oligocene andesite: *Lithos*, vol. 64, p. 63-75
- Peng, G.; Luhr J.F., and McGee J.J., 1997, Factors controlling sulfur concentrations in volcanic apatite: *American Mineralogist*, vol. 82, p. 1210-1224.

- Roden, M.K., Parrish, R.R., and Miller, D.S., 1990, The absolute age of the Eifelian Tioga ash bed, Pennsylvania: *Journal of Geology*, vol. 98, p. 282-285.
- Rollinson, H. R., 1993, *Using geochemical data; evaluation, presentation, interpretation*: New York, John Wiley & Sons, 352 p.
- Sall, J., Lehman, A., and Creighton, L., 2001, *JMP start statistics* (2nd edition): Pacific Grove, California, Duxbury, 191 p.
- Samson, S.D., Kyle, P.R., and Alexander, Jr., E.C., 1988, Correlation of North American Ordovician bentonites by apatite chemistry: *Geology*, vol. 16, p. 444-447.
- Samson, S.D., Patchett, P.J., Roddick, J.C., and Parrish, R.R., 1989, Origin and tectonic setting of Ordovician bentonites in North America: Isotopic age constraints: *Geological Society of America Bulletin*, vol. 101, p. 1175-1181.
- Schirnack, C., 1990, *Origin, sedimentary chemistry, and correlation of Middle and Late Ordovician K-bentonites: Constraints from melt inclusions and zircon morphology* [M.S. thesis]: Albany, State University of New York, 81 p.
- Shaw, G.J., Chen, Y-A., and Scott, J., 1991, Multiple K-bentonite layers in the Lower Devonian Kalkberg Formation, Cobleskill, N.Y. *Geological Society of America Abstracts with Programs*, vol. 23, no. 1, p. A-126
- Shaw, G.H. 2003, Trace element chemistry of individual apatite phenocrysts as a tool for fingerprinting altered volcanic ash layers: Assessing interbed and intrabed variation at local and regional scales. *GSA Bulletin*, vol. 115, p. 933-942.

- Smith, R.C., and Way, J.H., 1983, The Tioga ash beds at Selinsgrove Junction,: in *Silurian Depositional History and Alleghenian Deformation in the Pennsylvania Valley and Ridge: 48th Annual Field Conference of Pennsylvania Geologists*, p. 74-88.
- Smith, R.C., II, Berkheiser, S.W., Jr., and Way, J.H., 1988, The Bald Hill Bentonite Beds: A Lower Devonian pyroclastic-bearing unit in the Northern Appalachians: *Northeastern Geology*, vol. 10, p. 216-230.
- Streck M.J., and Dilles D.H., 1998, Sulfur evolution of oxidized arc magmas as recorded in apatite from a porphyry copper batholith: *Geology*, vol. 26, p. 523-526.
- Sun, S. S., McDonough, W. F., 1989, Chemical and isotopic systematics of oceanic basalts; implications for mantle composition and processes: in Saunders, A. D., and Norry, M. J., eds., *Magmatism in the Ocean Basins*, Geological Society Special Publications, 42, p. 313-345.
- Tucker, R.D., Bradley, D.C., Ver Straeten, C.A., Harris, A.G., Ebert, J.R., and McCutcheon, S.R., 1998, New U-Pb ages and the duration and division of Devonian time: *Earth and Planetary Science Letters*, vol. 158, p. 175-186
- Ver Straeten, C.A., 1992, A newly discovered K-bentonite zone in the Lower Devonian of the Appalachian Basin: Basal Esopus and Needmore Formations (late Pragian-Emsian): *Geological Society of America, Abstracts With Programs*, vol. 24, no. 7, p. A320.
- Ver Straeten, C.A., 1996, Stratigraphic synthesis and tectonic and sequence stratigraphic framework, upper Lower

and Middle Devonian, northern and central Appalachian Basin
[Ph.D. thesis]: Rochester, New York, University of
Rochester, 800 p.

Ver Straeten, C.A., 2001, Emsian-Eifelian (Lower-Middle
Devonian) of Virginia-West Virginia, and a basinwide
synthesis and sequence stratigraphy: Geological Society of
America, Abstracts with Programs, v. 33, no. 2, p. A61.

Ver Straeten, C.A., 2002, K-bentonites, ash bed preservation,
and implications for Lower to Middle Devonian volcanism,
Eastern North America: Geological Society of America,
Abstracts With Programs, vol. 34, no. 6, p. 135.

Ver Straeten, C.A., 2004, K-bentonites, volcanic ash
preservation, and implications for Early to Middle Devonian
volcanism in the Acadian orogen, eastern North America: GSA
Bulletin, v. 116, p. 474-489.

Ver Straeten, C.A., Monteverde, D.H. and Inners, J.D., 2001,
Stop 8. Fairway and U.S. 209 shale pit: Upper Onondaga
Limestone, Union Springs Formation, and basal Union Springs
decollement: in Inners, J.D. and Fleeger, G.M., eds., 66th
Annual Field Conference of Pennsylvania Geologists,
Delaware Water Gap, p. 232-243.

Waechter, J.W., 1993. Correlation of the Tioga Bentonites using
rhyolitic melt inclusions found in quartz phenocrysts as
geochemical fingerprints. Unpublished MS thesis, State University
of New York at Albany. 161 pp., +xvi

Waechter, J.W., Delano, J.W., Hanson, B.Z., 1993. Geochemical correlation of the Tioga Bentonites (Middle Devonian) using high-precision electron microprobe analyses of rhyolitic melt inclusions that occur in quartz phenocrysts: Geological Society of America, Abstracts with Programs, vol. 25, no. 6, p. 76